Escola de Camins
Escola Tècnica Superior d'Enginyeria de Camins, Canals i Ports
UPC BARCELONATECH

Hydro-mechanical characterisation of a mixture of sand/bentonite (80/20)

FINAL WORK OF MASTER

Work done by:
Cesarina Quezada García

Codirected by:
Antonio Lloret Morancho
Enrique E. Romero Morales
Clara Alvarado

Master in:
Geotechnical Engineering

Barcelona, 26 de Noviembre de 2020

Department of Civil and Environmental Engineering.

Table of Contents

List of Figures

List of Tables

Acknowledgements

This thesis would not have been possible without the support of many people.

I would like to start by thanking my supervisors Enrique Romero, Antonio Lloret, and Clara Alvarado for their guidance and support through this investigation. Thank you for giving me this opportunity to work on a challenging project, for the multicultural environment, and for the work in a dynamic team. Thank you for believing in me since we started this project, this means a lot to me.

I would like to thank my friends Rubí Vargas and Judith Landinez, for being there through all these processes, in the good and the bad times. Also for being available even in lab tests whenever I needed an extra hand because one person was not enough, especially in those compaction processes.

I am deeply thankful for Karolin Pujols and Manuel Marcano because from the beginning of this journey they were by my side, loving me in spite of the distance.

Great special thanks to Norbert Mezo for believing in me, and for providing tremendous support even in my bad days, through the whole process.

Special thanks to my parents Teofilo Quezada and Teresa García, without them I could not have become the person I am today. I would like to thank them for showing me how to live with morality and dignity, for teaching me that from all the things experienced in life we can always learn something and for not having doubt that I am capable of achieving my goals in these two years.

Abstract

Deep geological disposal system are being considered as a disposal of high level of radioactive waste. Part of the system consists in bentonite-based materials placed around the waste canister working as a barrier, ensuring the integrity of the storage. Bentonite have been considered as sealing material because of its properties including: low permeability, swelling pressure and others. Nowadays, sand is another material that is been considered due to its properties of isolation and heat dissipation. These materials experience drastic changes due to the radioactive decay of the waste, therefore it is important to characterise and understand the hydro-mechanical behaviour of these materials.

MX-80 granular bentonite and mixture sand/bentonite (80/20) materials have been evaluated in this investigation. The purpose is to know its hydro-mechanical behaviour and to seek a methodology to be able to emplace these material into a mock up (MU) cell, where transport with distilled water and gas tests will be carried out. Conventional oedometer test and swelling tests under constant volume are performed. The tests results indicate that the materials after being under load reduce its swelling behaviour, except in one of them where the optimum water content and a dry density higher than the dry density target is tested. The MX-80 bentonite shows more swelling pressure than the mixture sand/bentonite. This can happen due to the mineralogy of the pure bentonite. In addition, standard proctor tests were carried out, measurements of the water conductivity and suctions with different water content and similar densities were obtained. Three trial layer compaction tests were carried out in order to determine the best methodology of emplacement these materials into the cells, controlling their initials conditions.

Resumen

Los sistemas de almacenamiento geológicos a gran profundidad están siendo considerados como depósitos de residuos radioactivos de alto nivel. Parte del sistema consiste en materiales a base de bentonita colocados alrededor del recipiente que contiene los residuos funcionando como barrera, asegurando la integridad del almacenamiento. La bentonita se ha considerado como un material sellante debido a sus propiedades que incluyen: baja permeabilidad, presión de hinchamiento, entre otras. En la actualidad, la arena es otro material que se ha tomado en consideración por sus propiedades de aislamiento y disipación de calor. Estos materiales sufren cambios drásticos, debido a la desintegración radioactiva del residuo, por lo que es importante caracterizar y comprender el comportamiento hidro-mecánico.

En esta investigación se han evaluado los materiales MX-80 bentonita granular y arena/bentonita con una dosificación de 80/20. El propósito es conocer su comportamiento hidro-mecánico y buscar una metodología para poder colocar estos materiales en una celda prototipo de pruebas simuladas (MU) donde se realizarán ensayos de transporte con agua destilada y gas. Se realizan ensayos edométricos convencionales y ensayos de presión de hinchamiento a volumen constante. Los resultados de los ensayos indicaron que los materiales después de estar bajo carga reducen su comportamiento de hinchamiento, excepto en uno de ellos, donde el contenido de humedad óptimo con una densidad seca mayor a la densidad seca óptima es ensayada. La bentonita MX-80 muestra mayor presión de hinchamiento que la mezcla arena/bentonita. Esto puede suceder debido a la mineralogía de la bentonita pura. Además, se realizaron ensayos de proctor estándar, medidas de la permeabilidad y medidas de succiones con diferente contenido de agua y densidades similares. Se realizaron tres ensayos de compactación en capas con el fin de determinar la mejor metodología de colocación de estos materiales en las celdas prototipo, controlando sus condiciones iniciales.

1 Introduction

Due to the necessity, which arises through the years, to permanently locate high-level radioactive waste, deep geological radioactive waste deposits are considered and expansive clays act as barriers to these residues. Its purpose consists in storing those radioactive residues at a certain depth that prevents the migration of radionuclides into the atmosphere. Expansive clays when in contact with groundwater show certain properties that makes them suitable to be used as nuclear waste barriers. Some of these properties are the absorption, microporous structure, low hydraulic conductivity and plasticity of these properties lead to act as a barrier and restrict the movement of nuclides from the deposit, in case of a failure in the container. In addition to the expansive clays, the study of mixtures of bentonite with sand is also considered, because they increase the thermal conductivity, hence the heat dissipation.

The characterisation of materials is part of a project with the Swiss agency NAGRA (National Cooperative for the Disposal of Radioactive Waste), entitled *Laboratory Investigation of Two-Phase Transport in Sand-Bentonite Mixtures,* this is extremely important to define the geotechnical properties of the materials that will be used in the prototypes reduced scale gas injection, moreover this is essential for the long-term behaviour of engineering barriers.

This framework proposes a characterisation and evaluation of pure MX-80 granular bentonite and also the sand/bentonite mixture with a dosage of 80% sand and 20% bentonite received in barrels from NAGRA. In addition, it is required to find a procedure to mould, place and compact these materials within cells, called MU-B (Mock Up test B) and MU-A (Mock Up test A), to observe their hydro-mechanical behaviour. One of the cells will have a reduction factor of one third (1/3) to one another in order to be able to make correlations on a real scale, where the high-level radioactive waste will be. The study of these materials includes tests concerning the characterisation such as: hygroscopic humidity, grain size distribution by sieving the material, oedometers, standard proctor, Atterberg limits, paraffin to obtain the densities, and suction measurements. From the data acquired, the aim is to obtain parameters that later serve to create a methodology for placing these materials inside the two cells mentioned above where transport with both distilled water and gas tests will be carried out and their behaviour will be observed and evaluated. Due to the significance of the results obtained in this thesis I contribute as a co-author to the paper *Material characterisation on GAST experiment* to be presented in the Pan-American Conference on Unsaturated Soils.

(1)

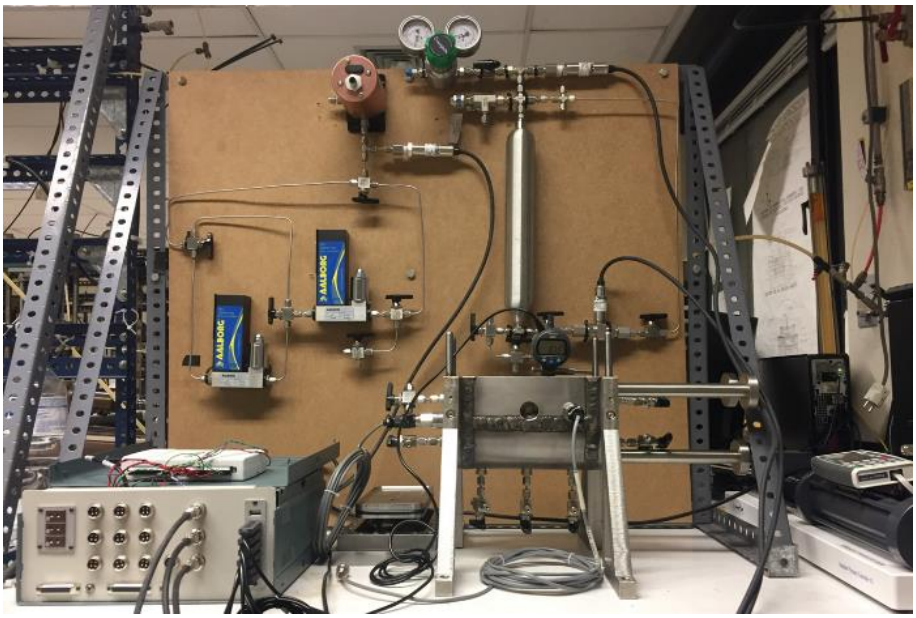

(2)

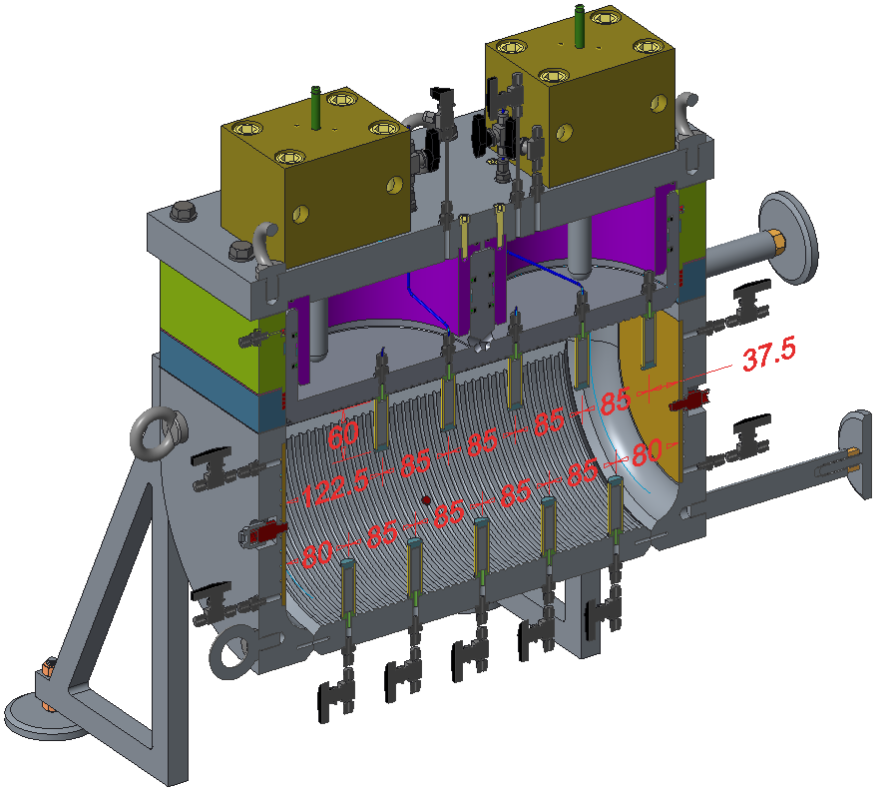

Figure 1.1. MU-B cell and equipment assembly (1). MU-A cell scheme (2)

1.1 State of the art

Bentonite-based materials are chosen as barrier materials in deep geological disposal of high-level radioactive waste. Bentonite provides a swelling pressure and low hydraulic conductivity to the barrier system giving long-term stability. These barriers/buffers perform important functions such as retarding the migration of radioactive nuclides in the atmosphere and preventing the entry of ground impurities towards the canister (Kale & Ravi, 2019). The use of sand/bentonite mixture is often preferred because of the increasing heat transfer and mechanical strength, as well as the isolation properties that the sand contributes to the bentonite (Cui, 2017).

In order to understand and quantify the behavior of these materials it is necessary to do an experimental characterisation of the bentonite-based materials. Different studies of bentonite and sand/bentonite mixtures have been carried out over the years depending on the scope of the investigation. One of those studies is taking into consideration the hydro-chemo-mechanical characterisation, focusing on water and gas transport properties through an 80/20 sand/bentonite mixture investigation made by Donatella Manca (2015). In this research the purpose is to ensure the safety of low and intermediate level of radioactive waste (L/ILW) repositories at both short and long terms, conducting an experimental characterisation of the mixture at macroscopic and microscopic level through water and gas injection tests. The response of the mixtures to chemical loadings revealed a strong dependency on the plastic limit to the salinity of the pore water. It is also revealed in this research that the swelling pressure and the saturated hydraulic conductivity depend on the applied matric suction and on the pore water chemistry, meaning that the mixture in contact with aqueous solutions loses most of its swelling capacity, causing an increment of the saturated hydraulic conductivity. In terms of the swelling capacity of the mixture, this remains low at a higher dry density, as well as the hydraulic conductivity. From a microstructural point of view the transition from double to single structure upon wetting was detected. On the other hand, the gas permeability of the mixture was independent from the compaction density (Manca, 2015).

Another report made by Seiphoori (2015) on bentonite-based materials develops the thermo-hydro-mechanical characterisation subject and combine it with modelling the bentonite studied which in this case is the Wyoming granular bentonite. This report was prepared on behalf of Nagra (National Cooperative for the Disposal of Radioactive Waste). In the macroscopic characterisation analysis of the Wyoming bentonite, it showed that static compaction upon water content does not influence the total suction, but it does in the total void ratio. The results obtained of the free swelling tests and final void ratio at a given suction has shown that about 40% of the final swelling capacity happens at last, when the suctions decrease and get to saturated conditions, this is observed in Figure 1.2.

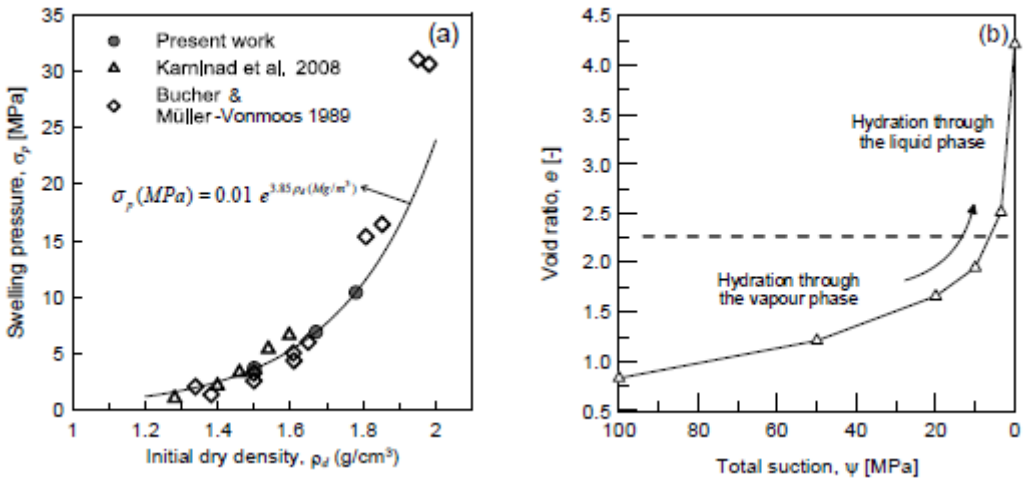

Figure 1.2. Swelling behaviour of Wyoming granular bentonite: (a) constant volume swelling pressure, and (b) free volume swelling vs total suction (Seiphoori, 2015)

The granular bentonite studied in this report was a mixture of different fractions of bentonite grains and aggregations. The compacted granular material shows a wide distribution of pore diameters with respect to the single grain. A macropore observation corresponding to the inter-aggregate porosity and a micropore network associated with intra-aggregate and intra-grain porosities are detectable for the as compacted granular bentonite. To determine the water retention curves a comparison between the retention behaviour of Wyoming bentonite, illite and kaolinite clays were presented, these materials were prepared at the same dry density of 1.80 Mg/m^3. The difference observed in Figure 1.3 among these materials was significant and it is associated with the different mechanisms that contributed to the water retention behaviour. The reason stablished in this report why the kaolinite mineral has a low retention potential is due to a capillary dominated behaviour within its structure. In MX-80 bentonite, the hydration of interlayer cations and the osmotic potential result in a high water retention capacity and the illite mineral behaves in between the other two clay minerals in terms of water retention behaviour (Seiphoori, 2015).

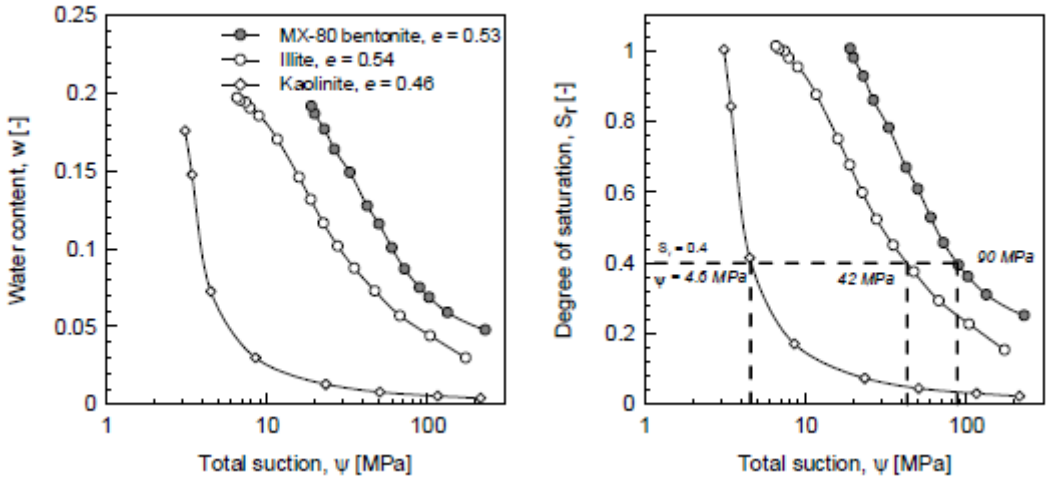

Figure 1.3. Water retention behaviour of Wyoming bentonite, illite and kaolinite (Seiphoori, 2015)

At the microscopic scale it is encountered that two mechanisms influenced in the water retention behaviour in bentonite, one of them is the hydration of the exchangeable cations (sodium) and the other is the osmotic attraction. The microstructural observation during the wetting and drying cycles for compacted bentonite samples indicated an irreversible change of the microstructure associated with the hydration state at the smectite particle level. The main difference stablished in this report between the microscopic and macroscopic behaviour of active and non-active clays is related to the existence of the active interlayer or nanopores (Seiphoori, 2015).

Other studies, for instance the research by Lloret, A. et al. (2003), have concluded that the suction has an important influence on the mechanical properties of the swelling material, affirming that the higher the suction is, the higher the yield stresses are going to be. The microstructure of the compacted expansive clay had a double structure made up of clay aggregates and large macrostructural pores. The pore space inside the aggregates was constituted of voids of a much smaller size. This bimodal structure it is also observed in others researches of clays Cui (2017), Villar & Lloret (2010), Romero (2013), Wang, Minh, Cui, & Delage (2013) moreover in bentonite pellet mixtures investigation of Hoffmann, Alonso, & Romero (2007). Although the microstructure and macrostructure mode of the sample is expected to be independent, the macropores depend on the dry density therefore it is important to mention that there is an influence of the microstructure on the macrostructure level, where it can induce important plastic strains. The changes in the microstructural level affect the macrostructural mode, however the changes in the macrostructural level do not influence the microstructural level.

Likewise a report about the thermo-hydro-mechanical characterisation by Villar (2005) gather information about the MX-80 bentonite with saline and deionised water. In this report the hydralic

conductivity was obtained taking into consideration the method of the fixed load permeameter and obtained compacting the bentonite at different dry densities. The results on this matter is presented in Figure 1.4, it shows that the hydraulic conductivity has an average 135 percent higher when water of 0.5 percent salinity is used as permeant. In this report is stated that if the values of the water conductivity are around 10^{-13} m/s, the difference is not significant.

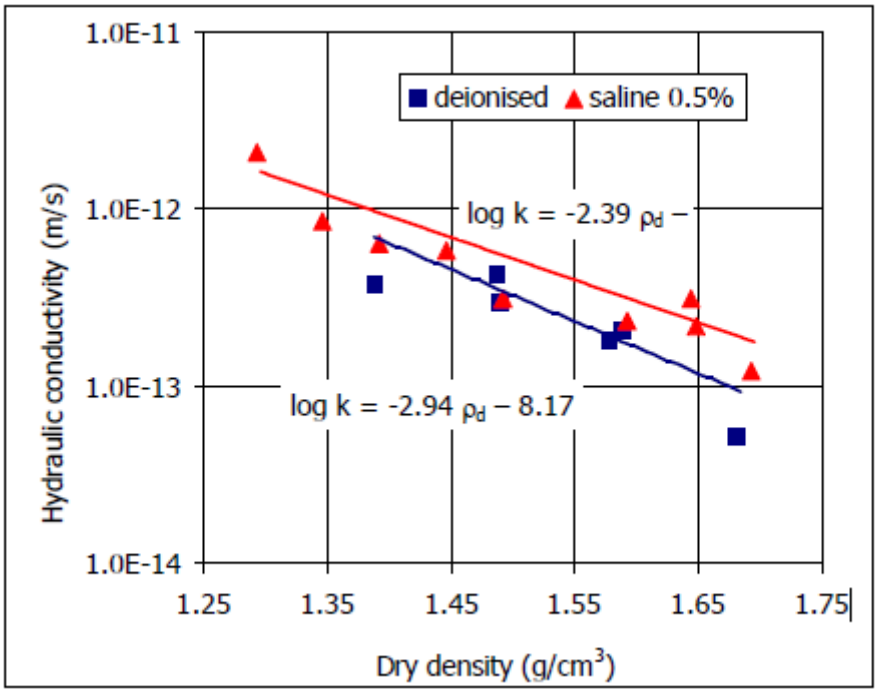

Figure 1.4. Results of the hydraulic conductivity tests with compacted MX-80 as a function of the kind of permeant (Villar, 2005).

1.2 Objectives and outline of the thesis

The aim of this investigation is to study the variability in the hydro-mechanical behavior that presents the Wyoming granular MX-80 bentonite and sand/bentonite. For instance, the performance of sand/bentonite is affected mainly by the dosage of bentonite used in the mixture. On the other hand, the behavior of the granular bentonite is affected by the water content, densification and among factors. Knowing these properties are important this is why the investigation has the following objectives:

- To characterise the Wyoming granular bentonite and the sand/bentonite (80/20), knowing their basics properties.
- To determine the saturated permeability.
- To accomplish swelling tests and determine the swelling pressure.
- To perform saturated oedometer tests to obtain the strain and permeability.

- To execute compaction tests to determine the most appropriate dry density and water content to place into the equipment (MU-B and MU-A).
- To seek a methodology to place and compaction the MX-80 granular bentonite and the sand/bentonite mixture (80/20) inside the two cells where later both distilled water and gas transportation tests are carried out.

1.3 Tested materials

The materials investigated are pure bentonite and sand mixture bentonite both of them are described below.

1.3.1 Wyoming granular bentonite

Wyoming granular bentonite known commercially as the brand MX-80 is used as a general term to describe clay formed by alteration of volcanic ash. The name comes from its existence which is in the Cretaceous Fort Benton unit in Wyoming, USA (Montañez, 2002).

To become the expansive clay chemical alteration of the ash has occurred in the presence of circulating mineral-rich groundwaters (Smellie & AB, 2001). The Wyoming bentonite includes any natural material dominantly composed of clay minerals in the smectite group, the presence of smectite mineral (more specifically montmorillonite) is considered as an active clay with swelling potential. Swelling bentonite contains a high concentration of sodium ions and will substantially increase in volume when it is wetted with water (Sutherland & Drean, 2014) .

The MX-80 is a sodium granular bentonite mainly composed of montmorillonite, quartz, muscovite, feldspar and calcite. This material more likely to be used in nuclear waste disposal. It has been considered as a buffer and as nuclear barriers in the construction of deep geological repository for deposition of high level radioactive waste (HLRW). These consideration is due to the special properties it presents when in contact with underground water, some of these properties include high swelling ability, low permeability, plasticity, absorption properties and good radionuclide retention ability which allows to restrict the movement of nuclides from the deposit (Akinwunmi, Sun, Hirvi, Kasa, & Pakkanen, 2019).

For the characterisation of the Wyoming granular bentonite, received in barrels by Nagra, the sample is taken without broken up the material. In order to select the material to use for its evaluation, a sieve analysis is made without altering (broke or smash) the sample given, thereby is chosen the material that passes through the sieve 0.4 mm containing coarse fractions and fine aggregate.

1.3.2 Mixture sand / bentonite (80/20)

The mixture used in this study, received by Nagra in barrels, contain grey quartz sand and Wyoming MX-80 bentonite in a proportion of 80/20 in dry mass. The specific gravity of the mixture is 2.67 (Manca, 2015).

The presence of sand with the bentonite help to transfer heat, the waterproofing capacity of the bentonite can be associated with the relatively high shear strength which is typical of the sand properties. The permeability of the mixture becomes very low, when the swell capacity of the bentonite exceeds the voids space available between the sand grains, thereby the pores are filled with hydrated bentonite (Proia, Croce, & Modoni, 2016).

The low permeability in a saturate state ensures that the principal transport mechanism in the barrier will be diffusion. On the other hand, the swelling pressure assures a self-sealing ability and closes gaps in the installed barrier (Sellin & Leupin, 2013). Therefore, the presence of sand in mixtures reduce the shrinkage of the mixture when the water content decreases and reduces the risk of cracking (Manca, 2015).

2 Basic properties of materials

This chapter covers the basics properties of pure bentonite and sand/bentonite (80/20).

2.1 Wyoming granular bentonite

To determine the basics properties of the pure bentonite, tests such as the Atterberg limits, hygroscopic water content and grain size distribution has been carried out. These tests are described below.

2.1.1 Hygroscopic water content

The hygroscopic water content described as the water absorbed from the atmosphere and is held by the soil particles is obtained for the material tested, being 6.43%. In Figure 2.1 it is observed how the material looked like when it arrived to the laboratory.

Figure 2.1. Wyoming granular bentonite in barrel

2.1.2 Grain size distribution

To prepare and know the pure bentonite for hydro-mechanical tests, a grain size distribution is made. The sieves, series ASTM, used were 7, 5, 4.55, 2, 1.20, 0.4, 0.150 and 0.074 mm, as presented in Figure 2.2. The procedure was determined by dry sieving at the hygroscopic water content (w% = 6.43).

Figure 2.2. Sieves for the grain size distribution test

After obtaining the grain size distribution of the MX-80 granular bentonite, presented in Figure 2.3, the calculated distortion number (CU) and the curvature number (CC) are determined and both are presented in Table 2.1. At plain sight the bentonite appeared to have various sizes of grains with bentonite powder.

The MX-80 bentonite will be placed in layers into two cells in order to work as a sealing material during the gas permeable seal test (GAST) and the transport with distilled water. Therefore, the material selected to this purpose is the one that passes through the sieve 0.4 mm. This procedure is made to eliminate the biggest bentonite pellets to provide better workability of the sample when doing the layers.

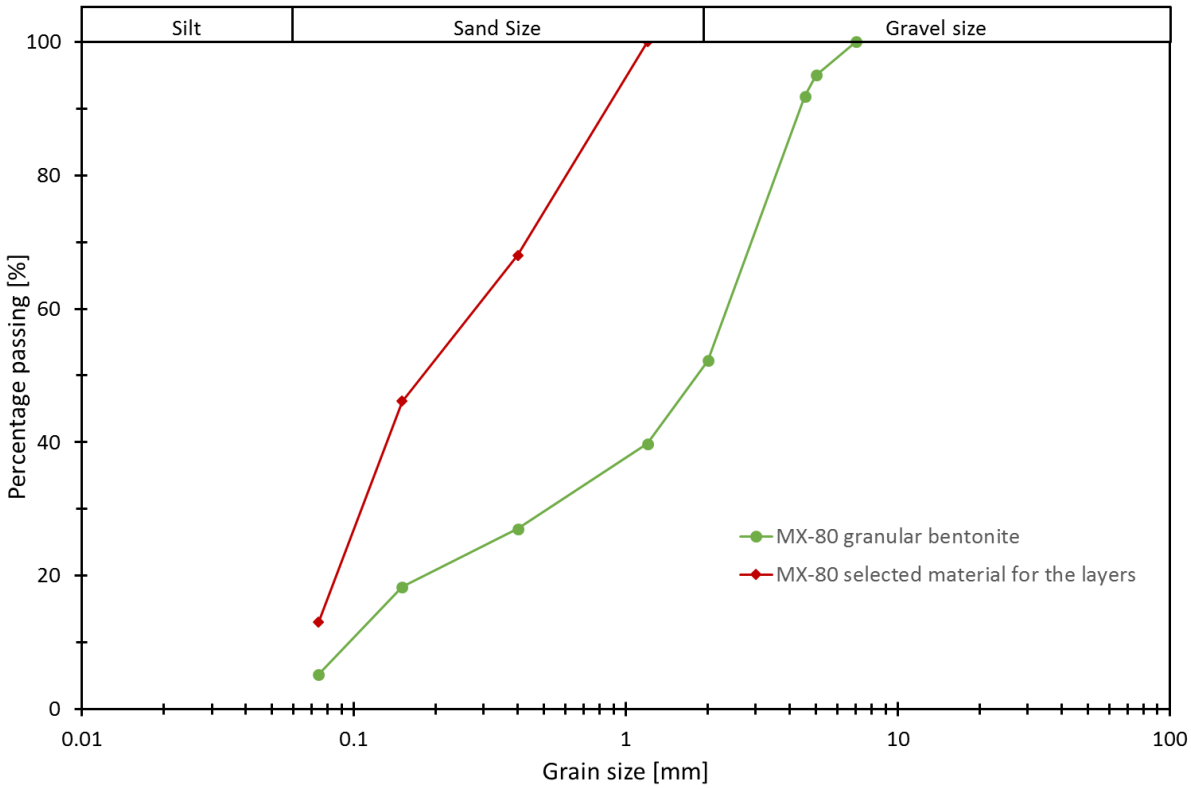

Figure 2.3. Grain size distribution MX-80 granular bentonite

Table 2.1. Uniformity coefficients and curvature number of pure bentonite tested in laboratory

	Granular bentonite
Uniformity coefficient (Cu)	16.83
Curvature number (Cc)	1.7

Figure 2.4. MX-80 bentonite before sieving with 0.4 mm

Figure 2.5. MX-80 after sieving with 0.4 mm

2.1.3 Atterberg limits

The Atterberg limits indicate the transition between the solid, plastic and liquid states, showing where a soil's physical behaviour changes. To determine the plastic limit (w_p) distilled water is used. The plastic limit is 65 % and was determined according to ASTM D4318.

Figure 2.6. Determination of plastic limit

The liquid limit was considered the same as stated in Seiphoori (2015), wl = 420 % measured using a fall cone penetration technique.

Table 2.2 contain a summary of the properties from the tests done to the Wyoming granular bentonite, it also includes a compilation of data from other works.

Table 2.2. Summary of general physical properties of the tested Wyoming granular bentonite

Smectite content [%]	Specific gravity *Gs*	Specific surface area *Ss* [m²/g]	Liquid limit w_l [%]	Plastic limit w_p [%]	Hygroscopic water content w_0 [%]
85*	2.74*	523*	420*	65	6.43

***** Seiphoori, 2015

2.1.4 Porosimetry

For the MX-80 bentonite material the porosimetry considered is bimodal defining intra-aggregate pores (micropores) and inter-aggregate pores (macropores) that depend on the dry density. To obtain these results the Mercury Intrusion Porosimetry (MIP) is carried out, taking into consideration the derivation of the Pore Size Distribution (PSD) function and the pore size diameter. These results are obtained by Seiphoori (2015) and it shows the behaviour when it is compacted with the initial conditions, a void ratio (e) of 0.53 and an initial water content (w_0) of 5%. The compacted state (A) presented in Figure 2.7 has two peaks with a modal value of 20 nm and 1.5 μm, this clearly shows a bimodal condition. The partially saturated state (B) S_r = 0.60 shows a decrease of the macropores volume but the same modal value, not showing important changes of the micropores. Finally, the fully saturated state (D) shows an important decrease of the macropores and an increase of the micropores due to the hydration of the material (Seiphoori, 2015).

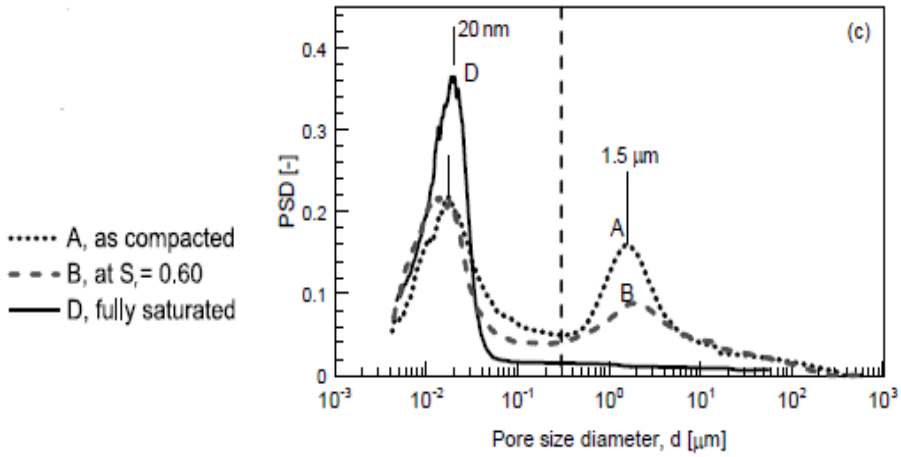

Figure 2.7. Pore size distribution during different phases (Seiphoori, 2015)

2.2 Sand/bentonite mixture (80/20)

To determine the basics properties of the mixture sand/bentonite (80/20), tests has been carried out, the results are presented below.

2.2.1 Hygroscopic water content

The hygroscopic water content of the mixture sand/bentonite (80/20) is 3.49%. This water content was determined to the sample as delivered. In Figure 2.8 it is presented the material as it arrived.

Figure 2.8. Sand/bentonite (80/20) in barrel

2.2.2 Grain size distribution

The grain size distribution is obtain by dry sieving at the hygroscopic water content (w% = 3.49) and is presented in Figure 2.9. The distortion number (CU) and the curvature number (CC) are listed in Table 2.3.

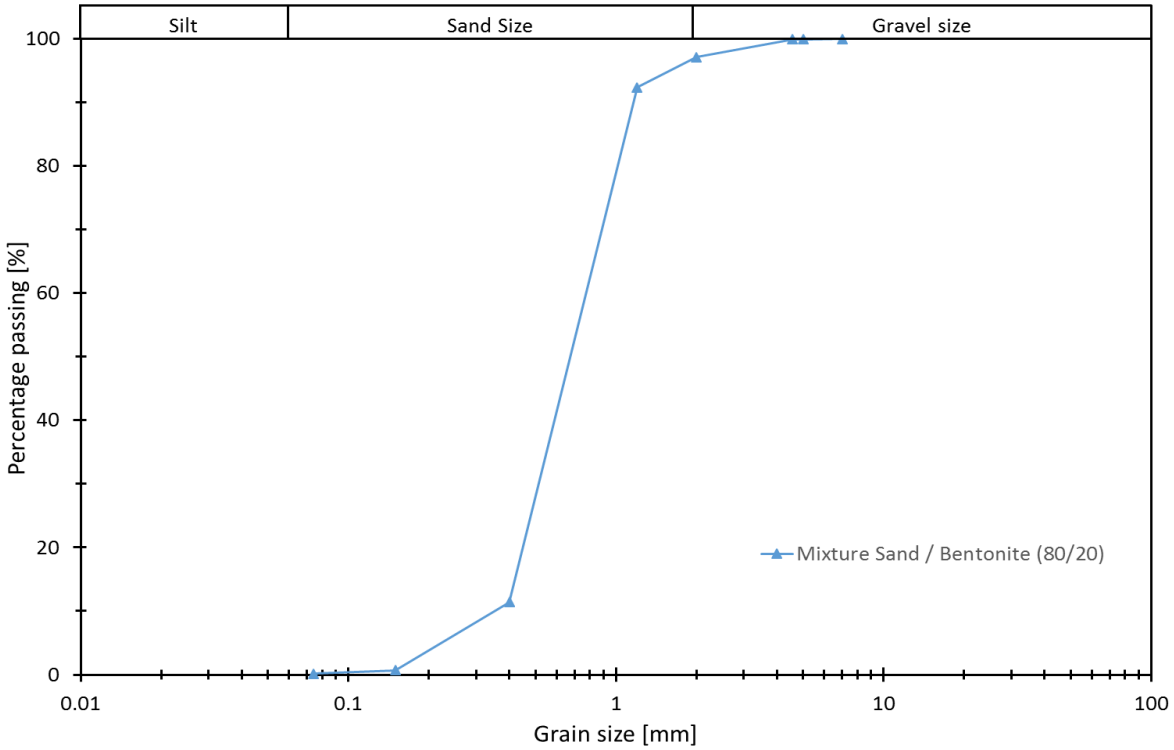

Figure 2.9. Grain size distribution mixture sand/bentonite (80/20)

Table 2.3. Uniformity coefficients and curvature number of pure bentonite tested in laboratory

	80/20 S/B
Uniformity coefficient (Cu)	2.51
Curvature number (Cc)	0.97

Table 2.4 contain a summary of the properties from the tests done to the sand/bentonite (80/20), it also includes a compilation of data from other works.

Table 2.4. Index properties of the mixture sand/bentonite (80/20)

Smectite content [%]	Specific gravity *Gs*	Specific surface area *Ss* [m²/g]	Liquid limit w_l [%]	Plastic limit w_p [%]	Hygroscopic water content w_0 [%]
17±	2.67±	105±	89±	23.5±	3.49

± Manca, 2015

2.2.3 Porosimetry

The same MIP test is carried out by Manca (2015) for the mixture sand/bentonite (80/20) and it shows that in the compacted state, the mixture has a bimodal pore size distribution (PSD). This test takes into consideration different dry densities between 1.43 Mg/m^3 and 1.79 Mg/m^3 and a water content of 11% with distilled water presented in Figure 2.10. The results show that distilled water at low dry densities 1.43 Mg/m^3 and 1.50 Mg/m^3 has a leading mode in the macroporosity region between 150 μm and 120 μm. However, at a higher dry density of 1.79 Mg/m^3 the leading macropores has a smaller pore diameter of 80 μm (Manca, 2015).

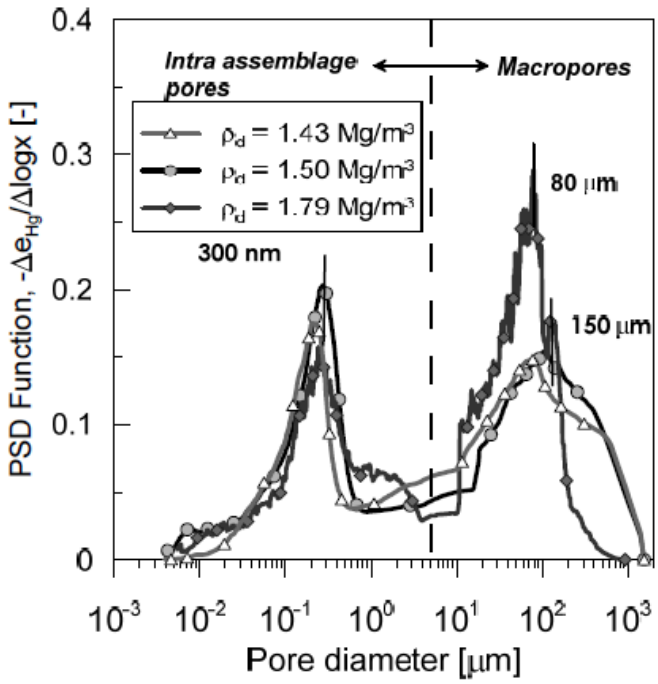

Figure 2.10. Pore size distribution with different dry densities (Manca, 2015)

Figure 2.11 shows a sample with a dry density of 1.5 Mg/m^3 that experience a reduction of the macropores due to wetting process under constant volume. It is appeared to be that the sample reduces the macropores to become a single structure by saturating and applying load. Moreover, Manca (2015) stated a single structure when the sample goes through a wetting and drying cycle.

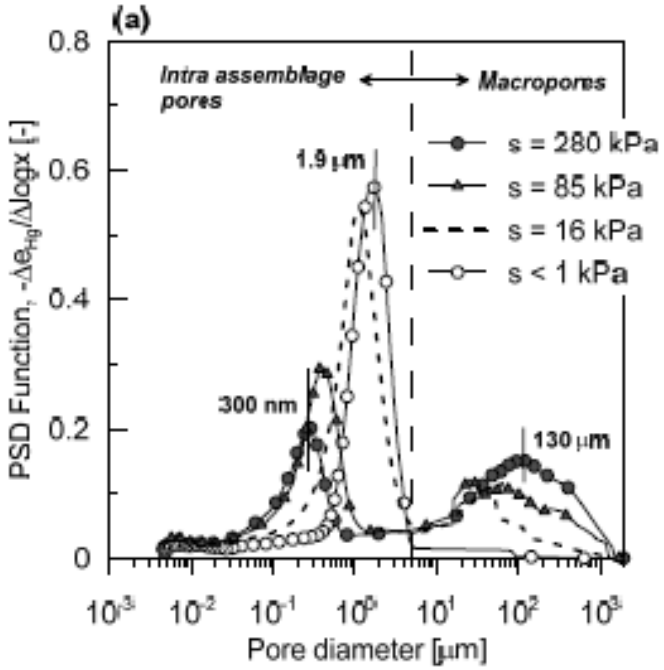

Figure 2.11. Pore structure evolution to wetting process under constant volume (Manca, 2015)

2.3 Summary and comparisons of the basics properties of Wyoming granular bentonite and sand/bentonite (80/20)

A summary of the several tests accomplished are presented below in Figure 2.12. Moreover, Figure 2.13 also shows the comparison of other studies to help characterised the materials better when the hydro-mechanical tests are executed.

By comparing the materials tested in the laboratory and other studies related to MX-80 granular bentonite, shown in Figure 2.13 and Table 2.5, it is observed that the MX-80 granular bentonite tested by González Blanco and Romero (2019) is the one with more similarities if the material would not be sieved by the 0.40 mm mesh. Taking into consideration the selected material was in fact sieved by 0.40 mm, the results obtained are more similar to the work of Manca (2015).

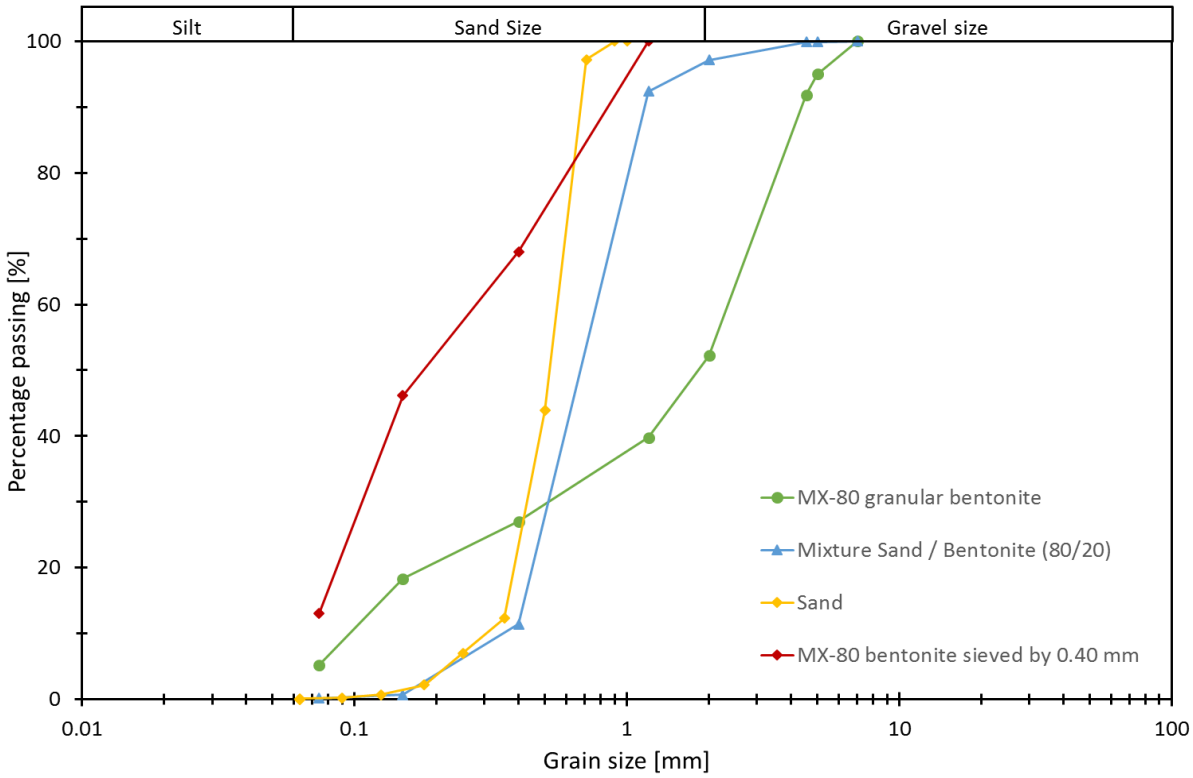

Figure 2.12. Grain size distribution of the materials tested

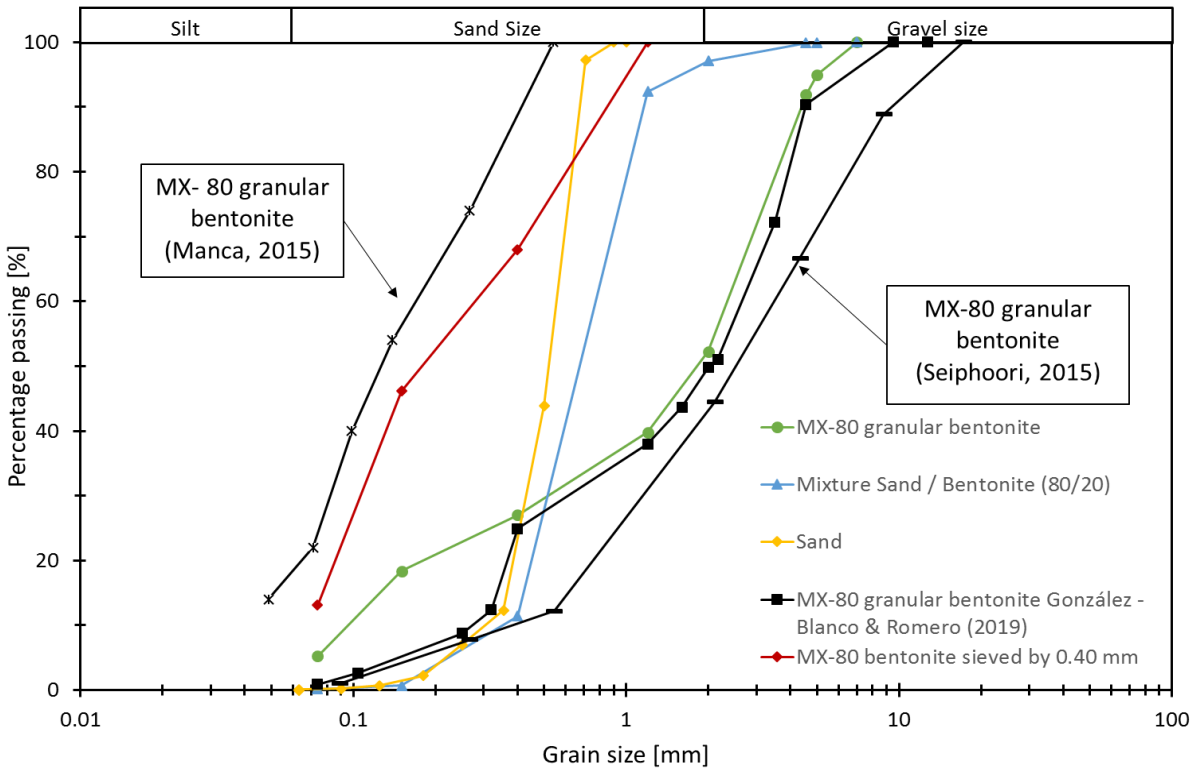

Figure 2.13. Comparison between other studies about MX-80 bentonite and the materials tested in the laboratory

Table 2.5. Summary of the uniformity coefficients and curvature numbers of the pure bentonite, the 80/20 S/B mixture and pure sand

Tested in Laboratory	Granular Bentonite	Bentonite sieved	80/20 S/B	100S
Uniformity coefficient (C_u)	16.83	5.19	2.51	1.87
Curvature number (C_c)	1.7	1.03	0.97	1.10
Seiphoori				
Uniformity coefficient (C_u)	11.04	-	-	-
Curvature number (C_c)	0.87	-	-	-
Manca				
Uniformity coefficient (C_u)	4.16	-	4.24	1.99
Curvature number (C_c)	0.88	-	2.54	1.19
González-Blanco & Romero				
Uniformity coefficient (C_u)	11.2	-	-	-
Curvature number (C_c)	0.55	-	-	-

3 Methodology on experimental hydro-mechanical tests for the characterization of the MX-80 bentonite and sand/bentonite

3.1 Dynamic compaction tests

The dynamic compaction of the samples were carried out in a small scale equipment with a hammer mass of 1.0 kg, a height of compaction stablished by 0.15 meter, a base and a sample compaction ring with a 50 mm diameter and a 20 mm thickness, shown in Figure 3.1. This compaction method was used to exert the conventional oedometer tests and the tests where the suction was measured.

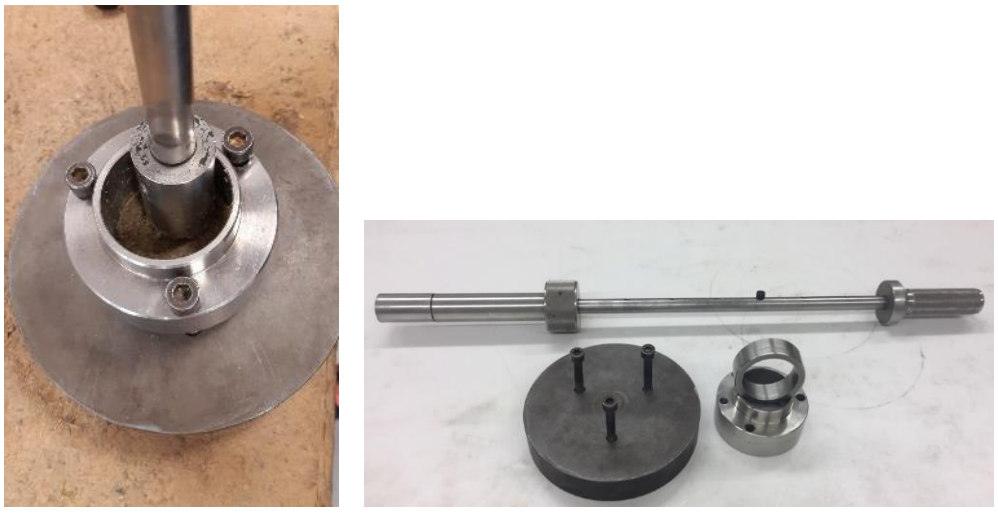

Figure 3.1. Dynamic compaction of the materials for the oedometer tests

3.2 Static compaction tests

The samples prepared for the swelling tests under constant volume conditions were statically compacted.

3.3 Standard proctor test

To obtain the compaction characteristics of the granular material in terms of optimum water content and maximum dry density a standard proctor test was carried out according to the ASTM D698-07. The five tests made were performed to the mixture sand/bentonite (80/20), where two of them were tested at the hygroscopic water content 3.49% and the other three at 11% of water content. The optimum water content with the corresponding maximum dry density were obtained by this test.

Figure 3.2. Standard proctor test to sand/bentonite (80/20)

In addition, to acquire the suction measurements and create the water retention curve, tests in compaction rings equal to the one used for the conventional oedometer tests were carried out. The height of the sample tested were 20 mm with a 50 mm diameter. These tests were performed taking into consideration the ASTM D698-07. Nevertheless, adjustments to the calculations, such as dimensions of the equipment, hammer mass, and others were made to obtain the energy of the proctor standard. In Figure 3.3 the equipment and method described is shown.

Figure 3.3. Compaction rings for conventional oedometer tests

3.4 Trial layer compaction and paraffin tests with MX-80 bentonite and sand/bentonite (80/20)

3.4.1 Trial layer compaction tests

In order to find a procedure to place and compact the mixture sand/bentonite and the pure bentonite inside the cells called MU-B and MU-A, it was performed three drafts layer tests. These tests were considered as a draft or prototype before definitely located these materials into the two cells for their evaluation.

The first trial made consist in the emplacement of the pure bentonite at the plastic limit water content to seek the best method of compaction and the behaviour of the material exposed to the environment and in contact with the mixture. For the emplacement of the materials a roller compaction was used presented in Figure 3.4.

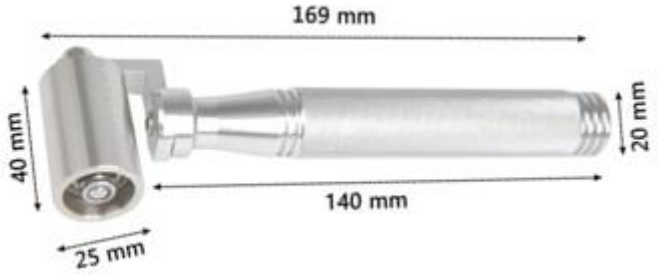

Figure 3.4. Roller compaction used to emplaced the MX-80 bentonite into the MU-B and MU-A

The mould used for the drafts was similar in shape to the MU cells, it has a diameter of 7.1 cm and a length of 13.9 cm. The height of the U shape considered for the pure bentonite prototype was 5.1 cm. Once the pure bentonite was compacted, the sand/bentonite mixture was next. The mixture was divided in two layers having 4.85 cm of total height with 11% of water content, both layers were dynamically compacted with a hammer mass of 1.0 kg. The thickness for the pure bentonite in the first attempt was 1 cm. By controlling the height and thickness of the materials, the dry densities target can be easily reached. This procedure it is observed in Figure 3.5.

Figure 3.5. Compaction procedure in a prototype mould with MX-80 bentonite and sand/bentonite mixture, first test

For the second test, the same methodology to emplace the materials was followed and the same prototype mould was used. In this case the pure bentonite was only emplaced and a paraffin test was carried out. The material was tested at a 71.83% of water content, greater than the plastic limit.

Figure 3.6. MX-80 bentonite with water content higher than the plastic limit, second test

For the third test, the materials were emplaced inside of the MU-B cell. This cell has a diameter of 10 cm and a length of 20 cm. The height of the U shape considered for the pure bentonite prototype was 4.65 cm. To place the materials and to be precisely in the height of every layer for each material a mould made by a 3D printer was used, this can be observed in Figure 3.7. For the MX-80 bentonite a mould of 5 cm wide and 23.66 cm length was used to compact the material and divide it into 4 strips outside the cell, to guarantee the dry density. The holes for the filter were consider when in making the layers.

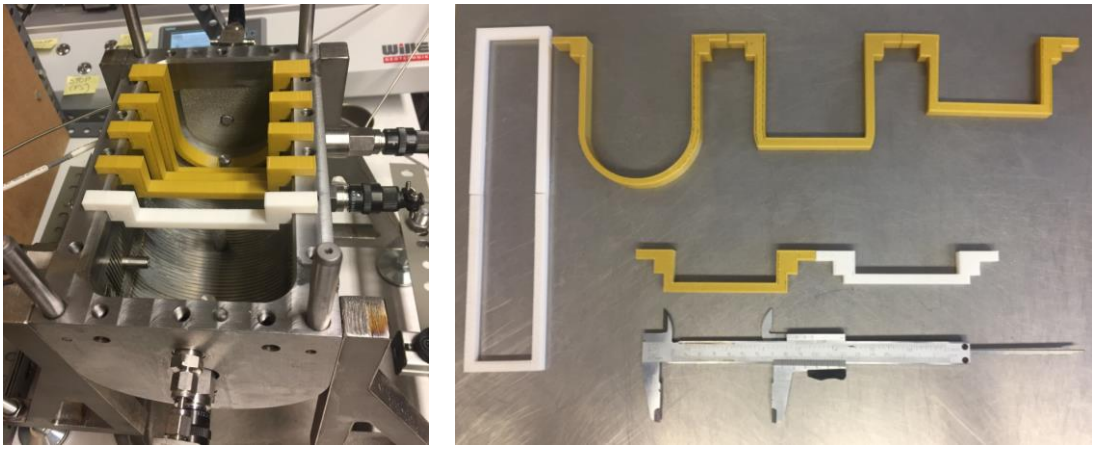

Figure 3.7. MUB-B cell with 3D printed moulds

On the third test a slice crystal mould and a plastic were used to avoid the strips to loose humidity and to control the weight of the material, as it shows in Figure 3.8, making sure that the material won't get stuck in the roller compactor.

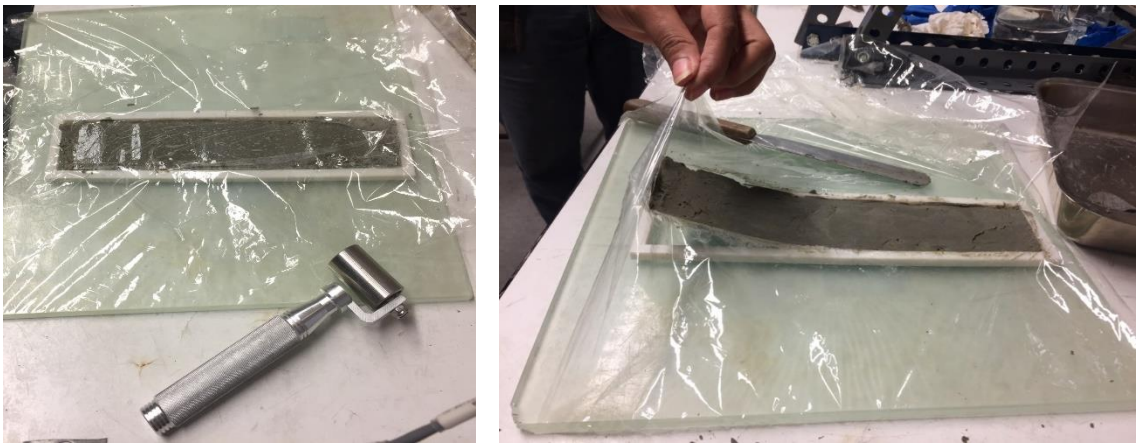

Figure 3.8. 3D printed mould for the MX-80 bentonite strips and slice crystal mould

Another mould was used after the strips were placed manually with a roller into the cells to guarantee the thickness of 0.7 cm inside of the cell. A humidifier was used to ensure that the water content remains the same these can be seen in Figure 3.9 and Figure 3.10.

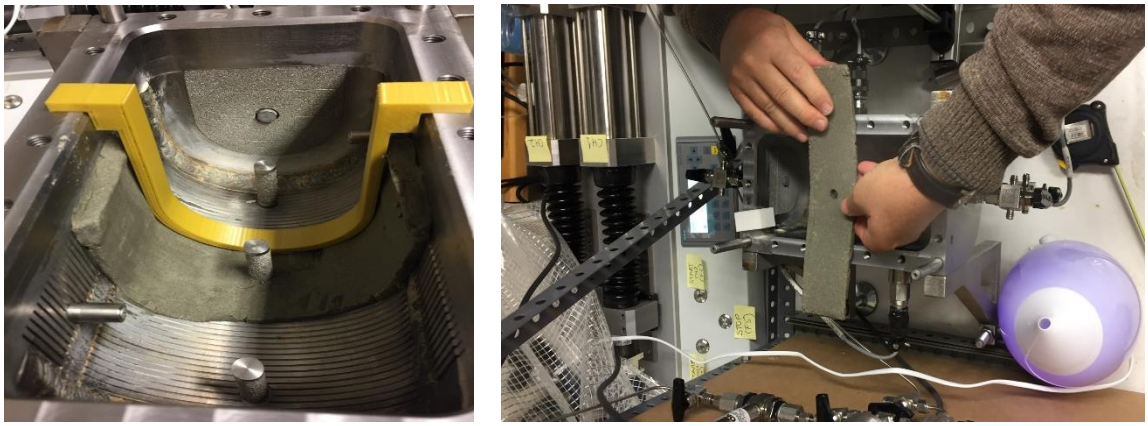

Figure 3.9. Placing the strips inside of the MU-B cell

The pure bentonite was again compacted by the roller inside of the equipment, making sure that there are no signs of cracked material and that is well attached to the equipment.

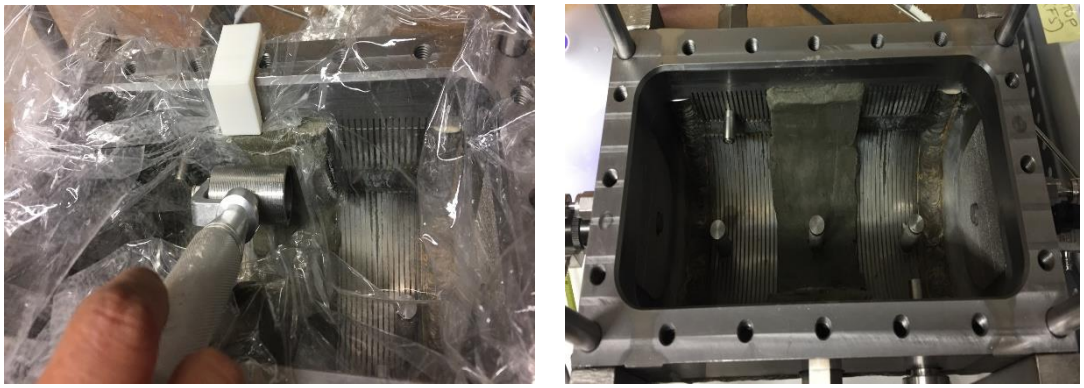

Figure 3.10. MX-80 bentonite compacted inside of the MU-B

In addition, the sand/bentonite (80/20) is dynamically compacted into 3 layers of 2.76 cm height. These heights are controlled by the moulds made by a 3D printed, as it is presented in Figure 3.11. The water content of the mixture was 11%. It must stand out that on the surface of the last layer of compacted sand/bentonite, a layer of bentonite with thickness of 0.7 cm is placed to work as a sealed of the mixture. For this test only the first layer of sand/bentonite was placed. The emplacement of both materials into the MU-B cell was taking well care of the filters and sensors that the equipment has.

Figure 3.11. Sand/bentonite placed inside MU-B cell.

3.4.2 Paraffin tests

To determine the bulk density of the compacted materials on the second and third draft tests made, molten paraffin is used. It is taken several samples from MX-80 bentonite and sand/bentonite (80/20). The procedure followed is described below:

1. It is obtained and weighted a small sample of the material without visible porosity.
2. Dip the samples into the melted paraffin and allow the excess to drain. Repeat this process until the paraffin covers and solidify the samples.
3. The weight of the sample with the paraffin is acquired.
4. The samples are immersed into water and the immersed weight is measure.
5. By knowing the density of the paraffin, the bulk density is achieved.

Figure 3.12. Paraffin test to a MX-80 bentonite

3.5 Oedometer tests

The oedometer tests were carried out to evaluate the consolidation characteristics of the Wyoming granular bentonite and sand/bentonite (80/20).

3.5.1 Conventional oedometer tests

The hydro-mechanical behaviour of MX-80 bentonite and sand/bentonite (80/20) will be analysed and interpreted under load conditions and compressibility in oedometric conditions which make it possible to study the one-dimensional compressibility of soils. For these tests the mixture sand/bentonite (80/20) was initially prepared at 11% of water content and then by dynamic compaction directly into the testing cell set to the target dry densities between 1.6 Mg/m^3 and 1.70 Mg/m^3. The sample dimensions after compaction had a height of approximately 10 mm, taking into consideration that it drains on both sides with a 50 mm diameter. The maximum load applied was 800 kPa.

After dynamically compacting the mixture, the samples were placed into a load arm oedometer system and the data was obtained by a LVDT as shown in Figure 3.13 and gathering the data in a program called GeoLab.

Figure 3.13. Conventional oedometer with load arm test for sand/bentonite (80/20)

The same methodology used for the mixture sand/bentonite is applied for the MX-80 bentonite to prepare the material into the sample compaction rings for the conventional oedometer tests. In this case, the pure bentonite was initially tested at 13.02%, 16.01%, 18.03% and 34.16% setting the target of dry densities between 1.10 Mg/m^3 and 1.30 Mg/m^3. The samples were emplaced into a conventional oedometer system without a load arm shown in Figure 3.14 . The maximum load placed was 75 kPa.

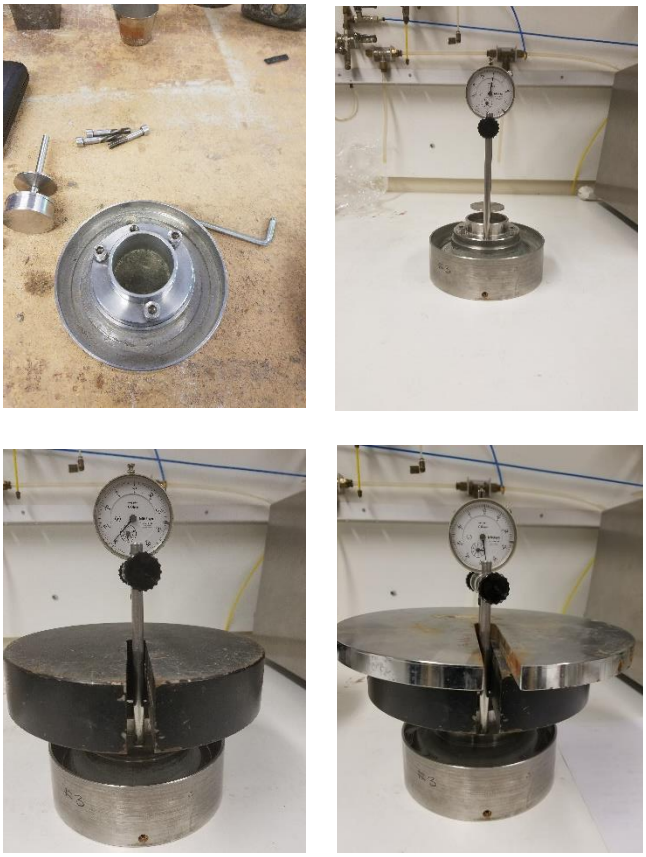

Figure 3.14. Conventional oedometer tests for MX-80 bentonite

3.5.2 Swelling tests under constant volume conditions

To determine the swelling potential of the materials sand/bentonite (80/20) and pure MX-80 bentonite a load cell is added to the oedometer equipment with a load arm shown in Figure 3.15. In this case the strain is controlled, to do so the load arm is fixed and the load cell measures the development of the swelling pressure (Lloret et al., 2003). The load arm has a loading ratio up to 1:20.

Figure 3.15. Load cell that measures the swelling pressure

In this investigation the swelling pressure of the materials restraining the changes of volume of the samples is studied. There were two samples tested of mixture sand/bentonite, one of them was carried using the oedometer load arm, however the other test was executed only with the load cell. The dry densities of the mixture tested were 1.64 Mg/m^3 and 1.78 Mg/m^3, and for the MX-80 bentonite the dry density was set to the target of 0.87 Mg/m^3. These samples were statically compacted directly into the testing cell which was then emplaced into the oedometer system or load cell presented in Figure 3.16. The sample dimensions for this test were 30 mm of diameter and 10 mm of height.

(1)

(2)

(3)

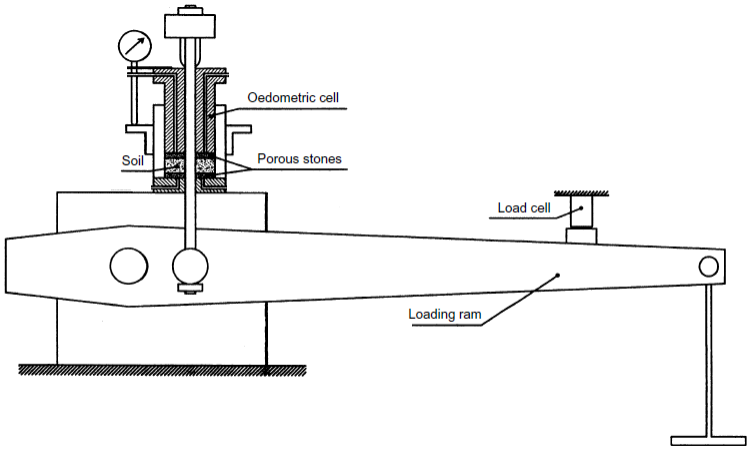

(4)

Figure 3.16. (1) Statically compacting the sample into the testing cell; (2) free swelling test under load with oedometer system using a load arm; (3) free swelling test only with load cell (4) Schematic oedoeter system by Lloret, A. et al. (2003)

3.6 Water retention curve

The water retention capacity is sometimes analysed by looking the soil curves that relate the liquid phase potential energy, expressed by total suction, to the amount of water retained in the material in terms of water content or degree of saturation (Seiphoori, 2015). The total suction, Ψ, is the sum of the matric, s, and the osmotic suction, π. For these tests the osmotic suction was not taken into consideration, sometimes this suction can be minor, and in other cases due to the bentonite ions and type of liquid used when in testing the materials, this suction can be larger. Having said that, in this framework the total suction will be considered the same as the matric suction.

To measure the suction a tensiometer INFIELD7 is used. This tensiometer is used to obtain the suction by capillarity. The limit of this tensiometer without having cavitation is from 0 to 200 kPa. The samples used the same ring cells that is used for the conventional oedometer tests. The sample dimensions after compaction had a height of approximately 20 mm with a 50 mm diameter. For the sand/bentonite (80/20) the water content is set to the target between 13% and 30%, meanwhile, for the MX-80 bentonite the water content is taken between 70% and 84%. The dynamic compaction was carried out in the same small scale equipment as the one used for the conventional oedometer tests. After compaction the next step is to measure the suction with the tensiometer as presented in Figure 3.17.

Figure 3.17. Measurements with a Tensiometer

4 Results analyses

4.1 Standard proctor test

The results of five tests made of sand/bentonite (80/20) are presented in Table 4.1. The optimum water content of 11% and corresponding dry density of 1.62 Mg/m^3 were obtained by this procedure.

Table 4.1. Results of the standard proctor test sand/bentonite (80/20)

Test	P1	P2	P3	P4	P5
Compaction energy (kJ/m^3)	585	585	866	1,170	1,684
Initial water content (%)	3.49	11	3.49	3.49	11
Bulk density (Mg/m^3)	1.54	1.80	1.58	1.59	1.90
Dry density (Mg/m^3)	1.49	1.62	1.52	1.53	1.71
Void ratio	0.789	0.643	0.751	0.742	0.557
Degree of saturation	0.12	0.46	0.12	0.13	0.53
Specific Gravity ±	2.67	2.67	2.67	2.67	2.67

±Manca, 2015

Figure 4.1 shows that the value obtained as optimum water content is the same acquired by Manca (2015). The dry density vary from the one stated in the work of Manca (2015) due to the energy applied.

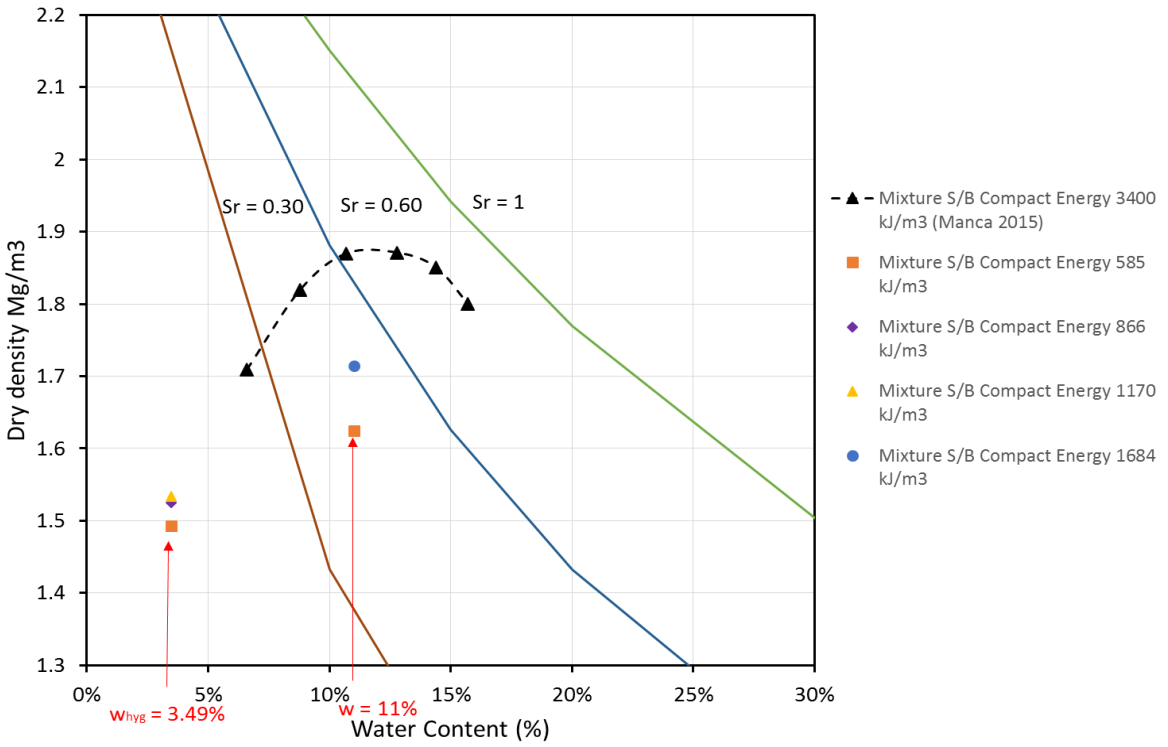

Figure 4.1. Compaction curve of the sand/bentonite (80/20) in a standard proctor test

In Figure 4.2 it can be seen that the more energy is applied to a sample with the same water content, the dry density will be higher.

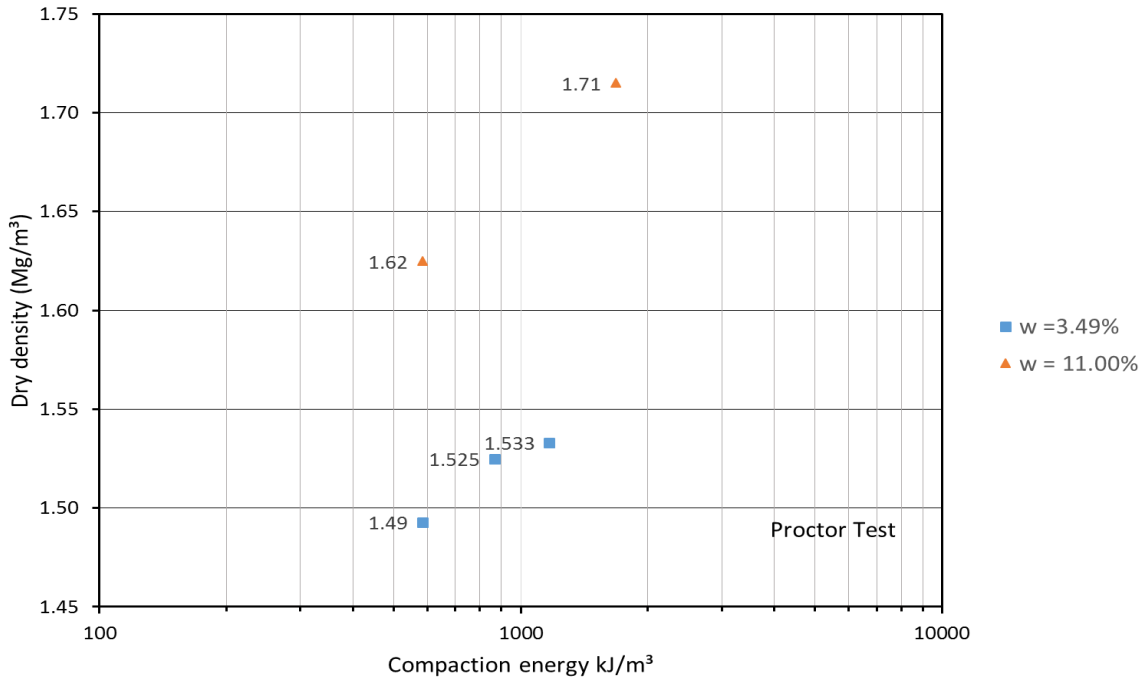

Figure 4.2. Dry density vs Compaction energy sand/bentonite (80/20)

4.2 Trial layer and paraffin tests of MX-80 bentonite and sand/bentonite (80/20)

Three tests in prototype mould were performed in order to determine the methodology to emplace the materials into the mock-up (MU) equipment, as well the optimum dry density and water content were defined. The results of the first trial test are shown in Table 4.2.

Table 4.2. First trial test results in prototype mould MX-80 bentonite

Test	1	2	3
Water content (%)	65.54	71.83	71.83
Bulk density (Mg/m³)	1.5⁺	1.38⁺	1.33⁺
Dry density (Mg/m³)	0.91	0.80	0.77
Initial void ratio	2.02	2.41	2.54
Initial degree of saturation	0.89	0.82	0.77
Specific Gravity*	2.74	2.74	2.74

* Seiphoori, 2015
⁺ Obtained with paraffin test

Figure 4.3 correspond to test 1. In this test it is observed how the material loses water content, moreover the cracks generated by compacting inside of the mould.

Figure 4.3. First trial test at 65% of water content MX-80 bentonite

Given that the mould adhesion is not guaranteed in test 1, new tests are performed with higher water content. For these tests, first the sample is compacted outside of the mould in a crystal plate and second, in order to avoid losing the water content and evade the sample to get stuck in the crystal, it is covered with 2 layers of plastic. As a result, the sample tested had no cracks and it was flexible to place in the mould, this can be observed in Figure 4.4.

From test 2, it is determined the optimum water content to place the material into the MU at 70% with a dry density of 0.87 Mg/m³.

Figure 4.4. Second trial test at 70% of water content MX-80 bentonite

The samples for the third trial test are placed in the MU-B equipment. In this test, 3D printed moulds are used to control the dimensions of the samples emplaced, as it is observed in Figure 4.5, allowing controlling the target dry density of MX-80 bentonite and sand/bentonite (80/20). To maintain the water content of the samples, a humidifier is placed near the MU-B equipment.

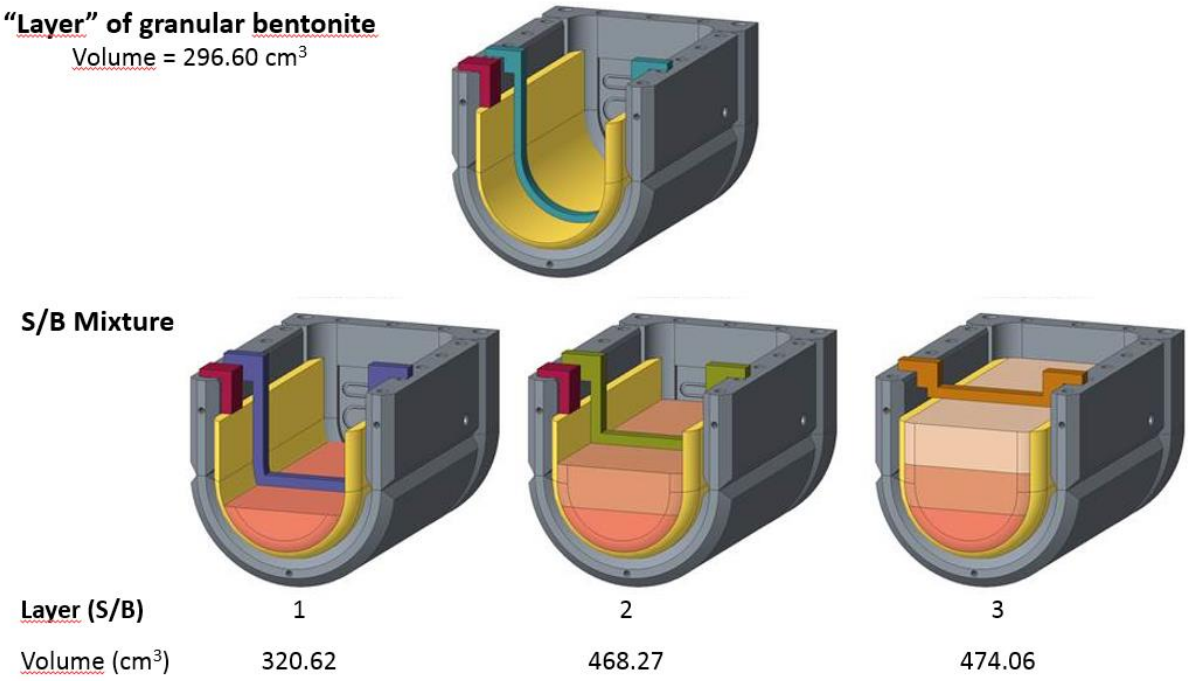

Figure 4.5. 3D printed moulds to control the volume of the sample placed in the cell

The MX-80 bentonite samples evaluated are extracted in three key points to have a better observation of the properties of the material placed as it is shown in Figure 4.6 . I1 correspond to the left side of the equipment, D3 to the right side and M2 to the middle. The results obtained are shown in Table 4.3.

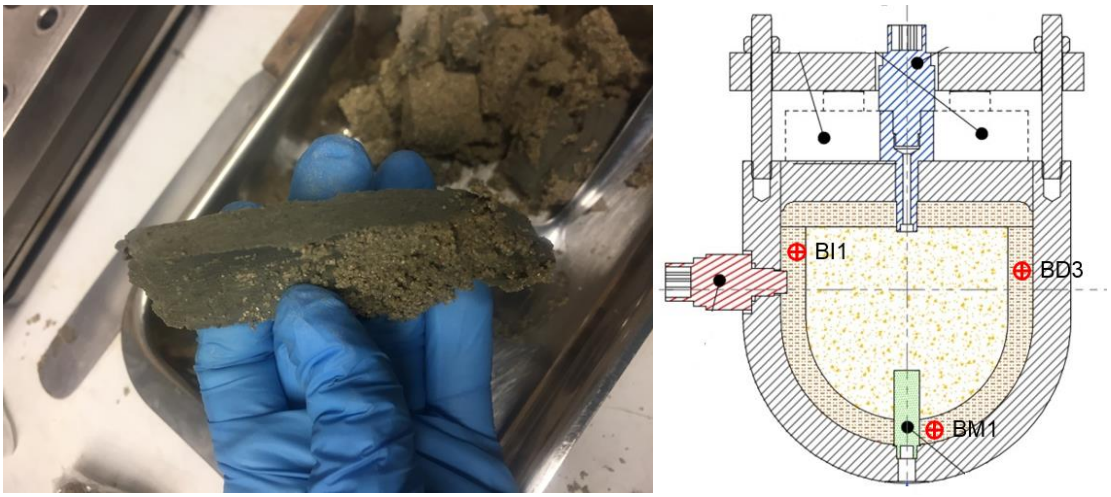

Figure 4.6. Extraction of MX-80 bentonite (right). Location of the samples extracted (left)

Table 4.3. Results third trial test in MU-B equipment of MX-80 bentonite

Test	I1	M2	D3
Sample depth (cm)	2	8.28	3
Water content (%)	66.27	59.34	63.82
Bulk density (Mg/m³)	1.58⁺	1.63⁺	1.62⁺
Dry density (Mg/m³)	0.95	1.02	0.99
Initial void ratio	1.81	1.62	1.70
Initial degree of saturation	0.96	0.96	0.99
Specific Gravity*	2.74	2.74	2.74

* Seiphoori, 2015
⁺ Obtained with paraffin test

Although the water content was reduced while the sample was prepared, the dry densities were higher than expected. In addition it is observed the material was without cracks and well joined to the equipment in Figure 4.7.

Figure 4.7. Third trial test with MX-80 bentonite emplaced in MU-B equipment

The sand/bentonite (80/20) is emplaced after the pure bentonite layer is fully compacted in the equipment. For this trial test only the first layer of the mixture was placed.

The samples evaluated are extracted in four key points to have a better observation of the properties of the material placed as it is shown in Figure 4.8. I1 correspond to the left and upper side of the layer emplaced, I2 to the left lower side, D1 to the right upper part and D2 to the right lower side of the layer. Results are shown in Table 4.4.

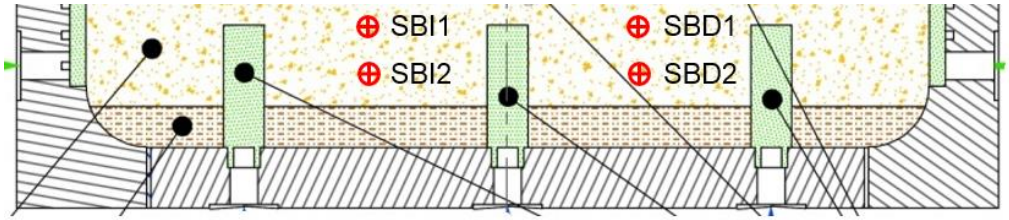

Figure 4.8. Extraction of sand/bentonite (80/20) (up). Location of the samples extracted (down)

Table 4.4. Results third trial test in MU-B equipment of sand/bentonite (80/20)

Test	I1	I2	D1	D2
Sample depth (cm)	0.69	2.07	0.69	2.07
Water content (%)	9.16	10.78	9.80	8.74
Bulk density (Mg/m³)	1.83⁺	1.88⁺	1.73⁺	1.66⁺
Dry density (Mg/m³)	1.68	1.70	1.58	1.53
Initial void ratio	0.59	0.57	0.69	0.75
Initial degree of saturation	0.42	0.50	0.38	0.31
Specific Gravity±	2.67	2.67	2.67	2.67

±Manca, 2015
⁺ Obtained with paraffin test

Despite the reduced of water content, as it happened in the process of emplacing the bentonite material, the target dry densities for the mixture were reached, except for the tests D1 and D2, which happened to be in the right upper and lower side of the equipment. Figure 4.9 shows when the mixture is fully compacted.

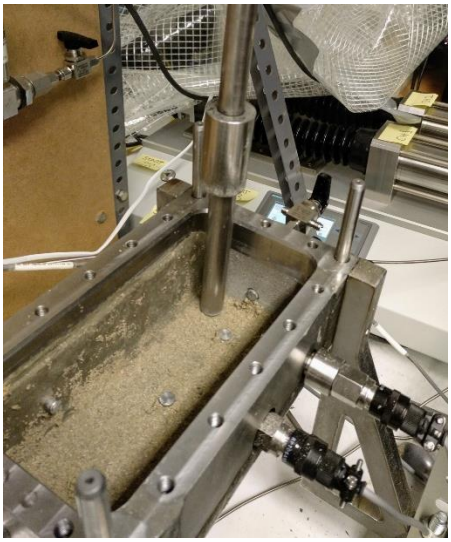

Figure 4.9. Third trial test with sand/bentonite (80/20) emplaced in MU-B equipment

4.3 Conventional oedometer tests

4.3.1 MX-80 bentonite

Table 4.5 includes the initial conditions of the tests that were carried out on cylindrical specimens directly in the oedometer cells.

Table 4.5. Initial conditions conventional oedometer MX-80 bentonite

Test	1	2	3	4
Water content (%)	13.02	16.01	18.03	34.16
Bulk density (Mg/m³)	1.47	1.55	1.30	1.44
Dry density (Mg/m³)	1.30	1.34	1.10	1.44
Initial void ratio	1.11	1.05	1.48	1.56
Initial degree of saturation	0.32	0.42	0.33	0.60
Specific Gravity*	2.74	2.74	2.74	2.74

* Seiphoori, 2015

The values of the initial voids are related to the soil structure when the minerals of montmorillonite are in contact with water. Clay minerals are characterise by high deformability on hydration. On the other hand, the values of the initial degree of saturation imply the presence of suction. The estimations of these suctions are presented in Table 4.6 and were made according to the characterisation curve for soils with different texture by Perez (2008).

Table 4.6. Initial values of suctions estimated

Test	1	2	3	4
Water content (%)	13.02	16.01	18.03	34.16
Initial degree of saturation	0.31	0.40	0.32	0.58
Initial Suction (MPa)	72.00	42.00	72.00	7.80

The deformation was prevented with a load of 50 kPa, in order to stabilise the deformability of the material. The other load of 25 kPa was applied after the saturation of the sample was guaranteed as shown in Figure 4.10. In this figure the material to be stable before the saturation phase is observed. The test with 65% of water content was not saturated. Part of the shrinkage presented in some of the cases is due to the movement that can happen nearby where the oedometers were placed. After deionise water is introduced, the sample shows a swelling behaviour. The behaviour is slightly reduced after applying the additional 25 kPa, except in test 4. This test stops its swelling behaviour when the load is applied then after two days the sample began to swell again. The experienced behaviour can be explained by the fact that the water pressure had not dissipated by the moment the load was applied.

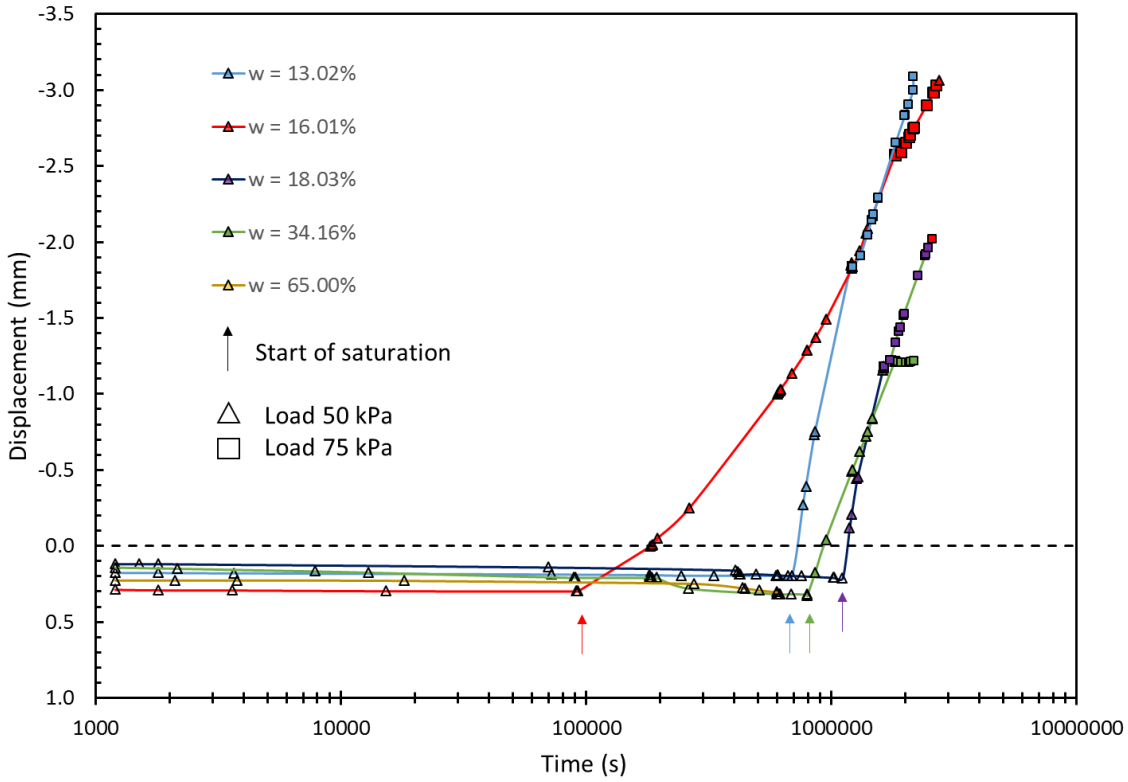

Figure 4.10. Displacement vs time for MX-80 bentonite conventional oedometer

The Figure 4.11 shows the development of void ratio in time. It is observed that the higher the initial water content is, the higher initial void ratio is. The test with 16.01% of water content, shows a minor void ratio than the test with 13.02% of water content, this could be affected by the energy applied during compaction. According to this figure the development observed during time indicates that the sample with least water content is the one with more swelling deformation.

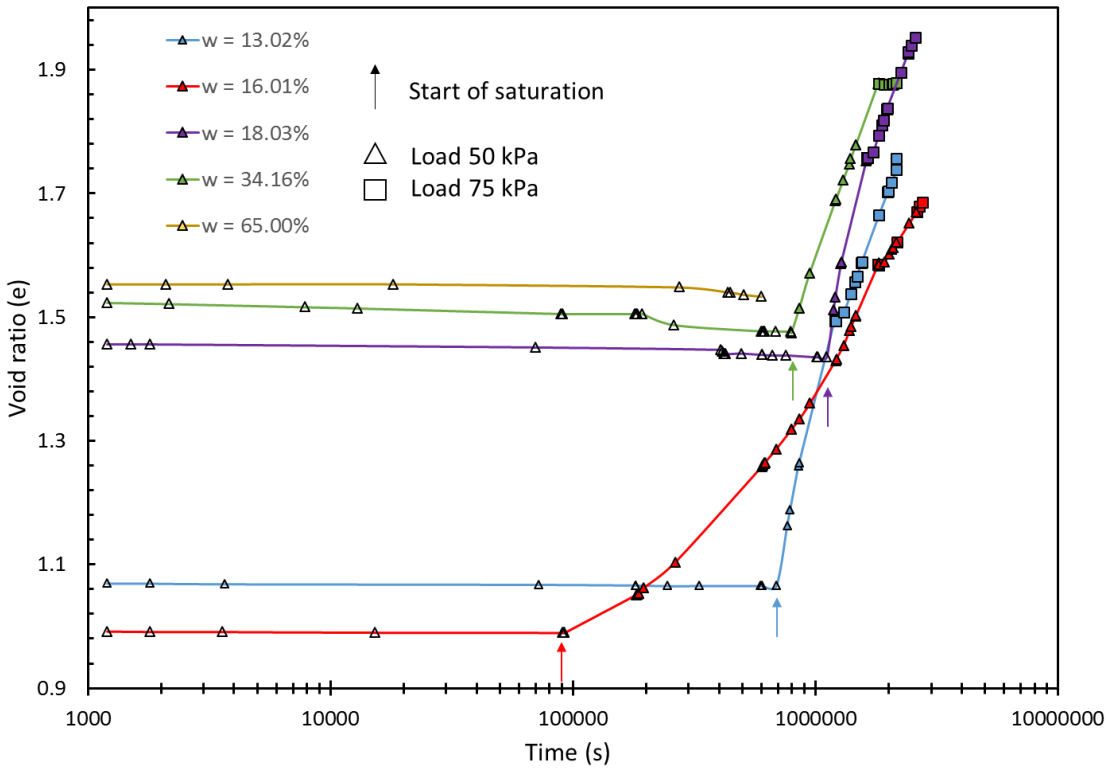

Figure 4.11. Void ratio vs time for MX-80 bentonite conventional oedometer

In Figure 4.12 the sample that has the lowest water content is the one that has the greater swelling strain percent.

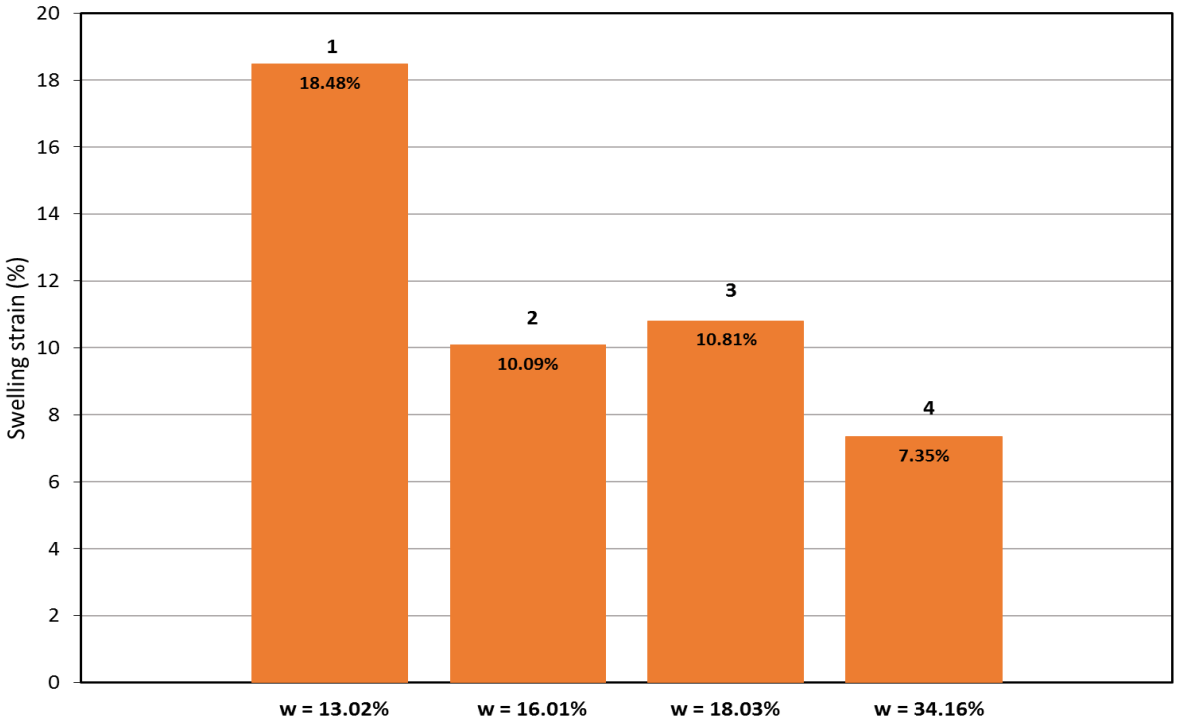

Figure 4.12. Swelling deformation at 6 days under 50 kPa load MX-80 bentonite

Comparing the Figure 4.13 and Figure 4.14 it is observed that the test 1 and 2 had the greater swelling strain and had at the same time the greater dry densities. The swelling strain in both tests are the highest because of the lowest water content that the samples had, meaning that when the samples were saturated, test 1 and 2 could adsorb more water in their crystalline lattice allowing these samples to expand more than the others.

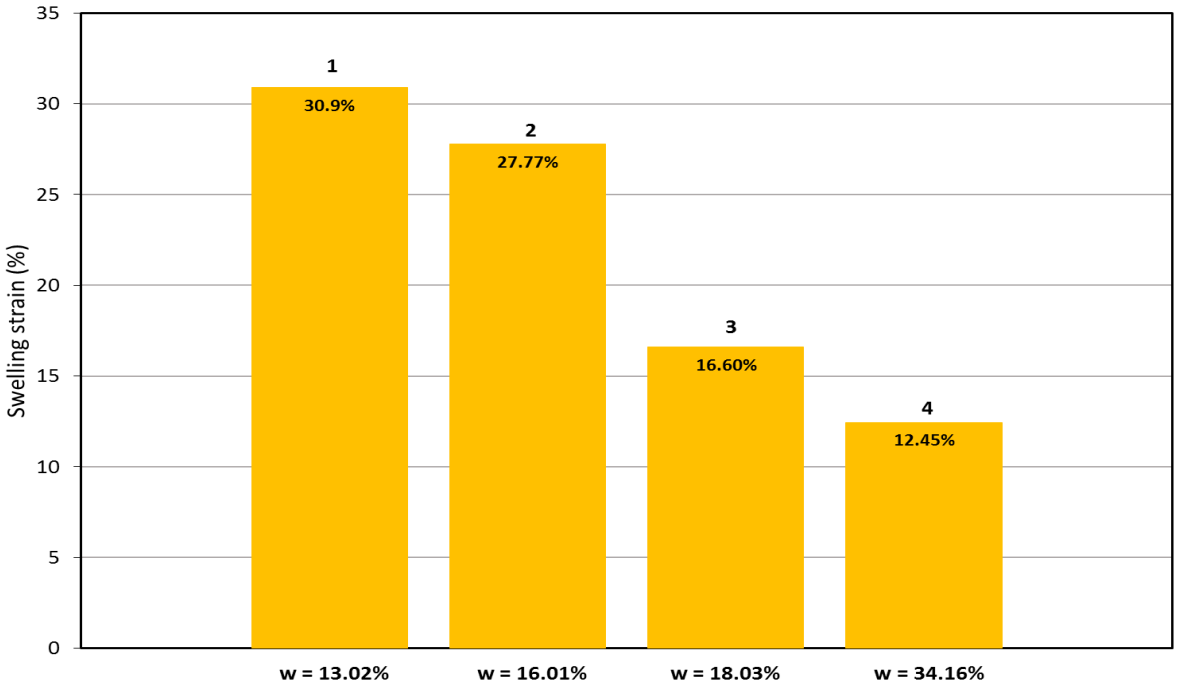

Figure 4.13. Swelling deformation at 4 days under 75 kPa load MX-80 bentonite

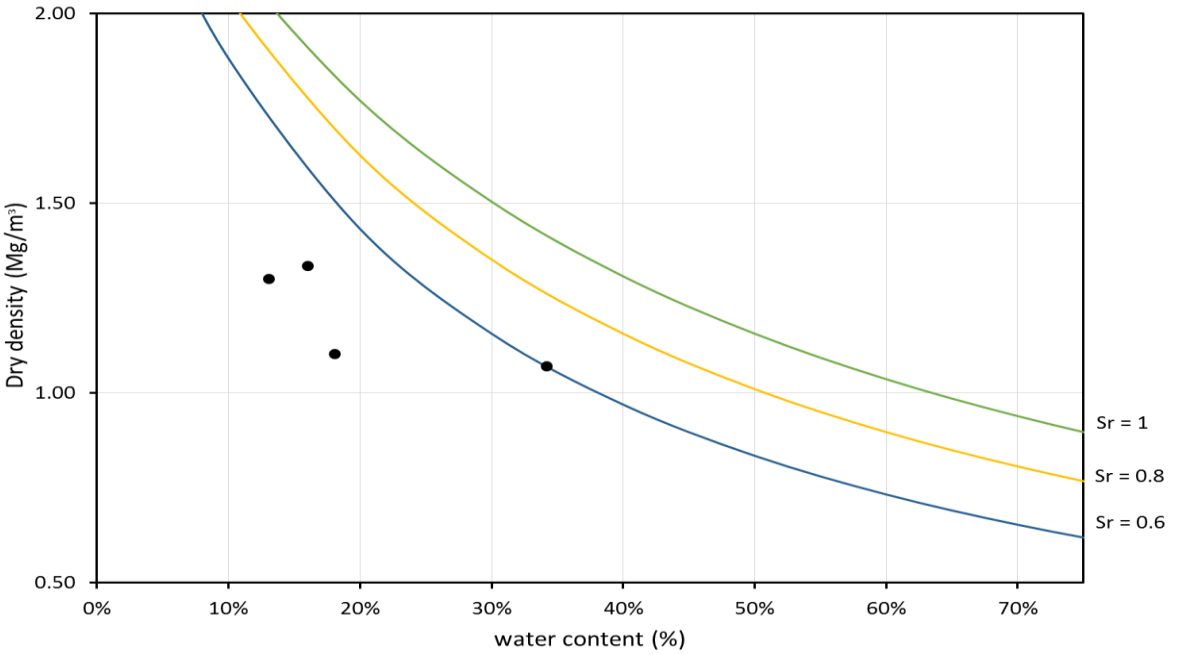

Figure 4.14. Dry density vs water content conventional oedometer MX-80 bentonite

A comparison between the results acquired and with other investigations are presented in Figure 4.15. This comparison shows the variability of the values of dry density that other investigations reported. The values obtained with the conventional oedometers are similar to the works of M. V. Villar & Lloret (2008) y Imbert & Villar (2006) with powder.

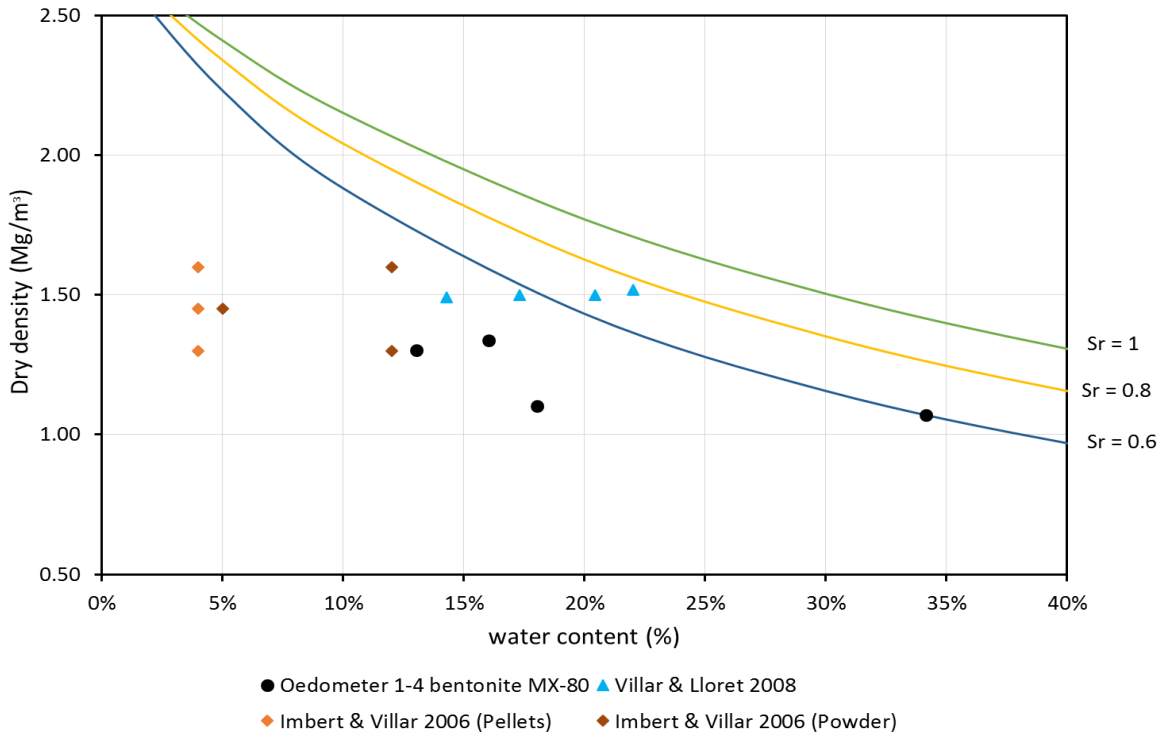

Figure 4.15. Dry density vs water content MX-80 bentonite results compared with other works

4.3.2 Sand/bentonite (80/20)

The path followed by these tests started with a loading of 50 kPa, then the sample is saturated, after that the material is loaded until 800 kPa and finally the unloading path of the sample occurs. The initial conditions of the three oedometers tests with a load arm are presented in Table 4.7.

Table 4.7. Initial conditions conventional oedometers S/B

Test	OE1	OE2	OE3
Compaction energy (kJ/m³)	266	304	342
Initial water content (%)	3.49	12.19	11.88
Bulk density (Mg/m³)	1.66	1.78	1.89
Dry density (Mg/m³)	1.61	1.58	1.69
Void ratio	0.663	0.687	0.581
Degree of saturation	0.14	0.47	0.55
Specific Gravity ±	2.67	2.67	2.67

±Manca, 2015

It is noted that the test OE1 was carried out with hygroscopic water content. In addition test OE3 has more energy of compaction applied, as a results this test has the higher dry density and the lowest void ratio.

The Figure 4.16 presents the results of the vertical strain in test OE1. After the 50 kPa load is applied, the sample increases its volume. It can be observed that under the load of 50 kPa, after soaking, the sample potentially starts to swell and a day after the saturation the material is stabilised. The more load is applied to the material, it is observed that the sample reduces its volume drastically, exceeding the pre-consolidation load. Once the unloading happens, the material tries to get back to its initial state, but only regaining approximately 22% of its initial height.

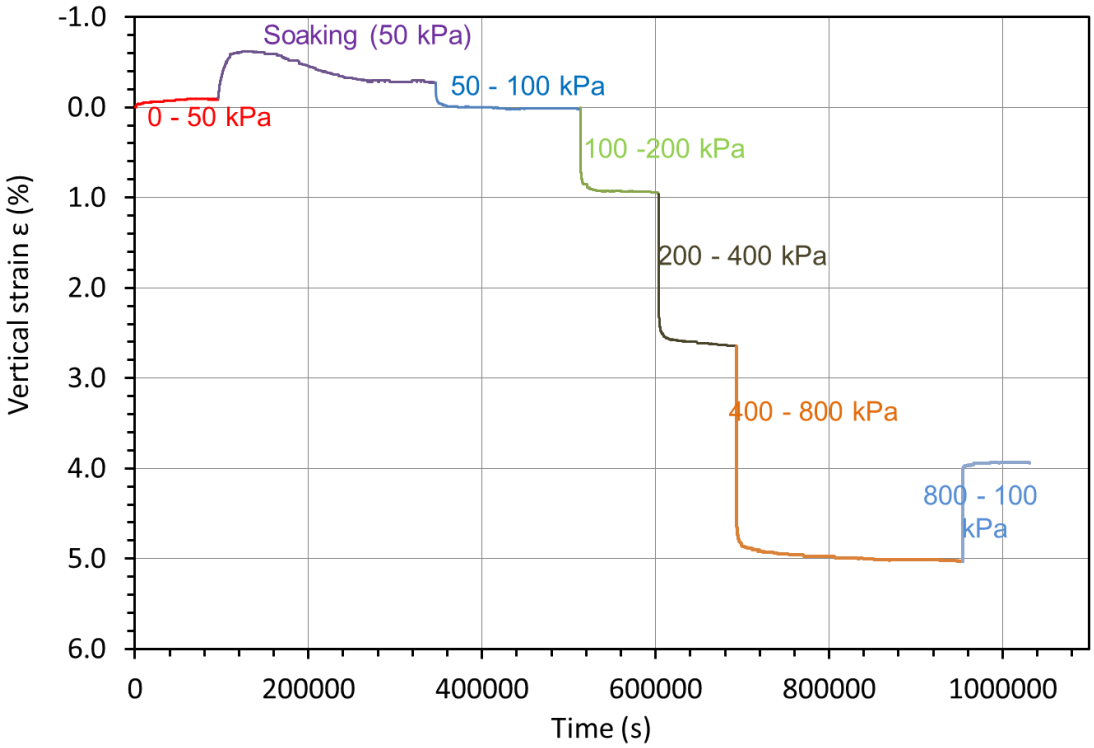

Figure 4.16. Vertical strain vs time for sand/bentonite (80/20) OE1 conventional oedometer test

Table 4.8 presents the properties of the materials indicating that the more compacted is the sample, the lowest is the permeability. Moreover, it is observed that the greater the modulus edometric is, the lowest the permeability will be, indicating soil stiffness. It can be seen, by the results above that the permeability is around 10^{-11} m/s at the beginning of the test and with the last load applied, the permeability gets lower.

To obtain a correction of the water conductivity, secondary consolidation and the consolidation coefficient values, a backanalysis was made taking into consideration the equation (1) shown below:

$$d = d_0 + \frac{2h}{Em} \Delta\sigma'_v \, \overline{U}(t, C_v) + 2hC_\alpha \log\left(\frac{t}{t_{90}}\right) \quad (1)$$

d_0 = Initial settlement
h = height of the sample
Em = modulus edometric
Ū = degree of consolidation
$\Delta\sigma'_v$ = effective stress
t_{90} = time at 90% consolidation
C_α = secondary consolidation
C_v = consolidation coefficient

The same equation was applied to OE2 and OE3.

Table 4.8. Properties of the material OE1 under load

Load step (kPa)	Average void ratio e	Average ρ_d (Mg/m^3)	c_v (10^{-8} m^2/s)	Edometric Modulus E_m (MPa)	C_α (10^{-4})	Water conductivity K (m/s)
50-100	0.656	1.61	4.7	30	0.0005	1.57E-11
100-200	0.646	1.62	2.0	26	0.0007	7.69E-12
200-400	0.624	1.64	2.8	29	0.0009	9.66E-12
400-800	0.591	1.68	3.4	40	0.0012	8.54E-12

The Figure 4.17 shows the behaviour of the sample OE2 under load through time. In this figure it is appreciated how the material expands after the unloading occurs. The material is trying to go back to its initial state, having an irreversible change of volume. In expansive soils after the loading and unloading cycling of a sample the swelling behaviour reduces. However, if a load applied exceed the preconsolidation stress of the soil, the results will show plastic deformations. Comparing OE1 with OE2 it is observed the material is more compressible in OE2 because of the water content in OE2 is greater than in OE1. In OE1 the sample was at hygroscopic water content, the microstructure could be changed when compacting the sample by the dry branch, which can also explained the difference in the swelling behaviour compared to OE2.

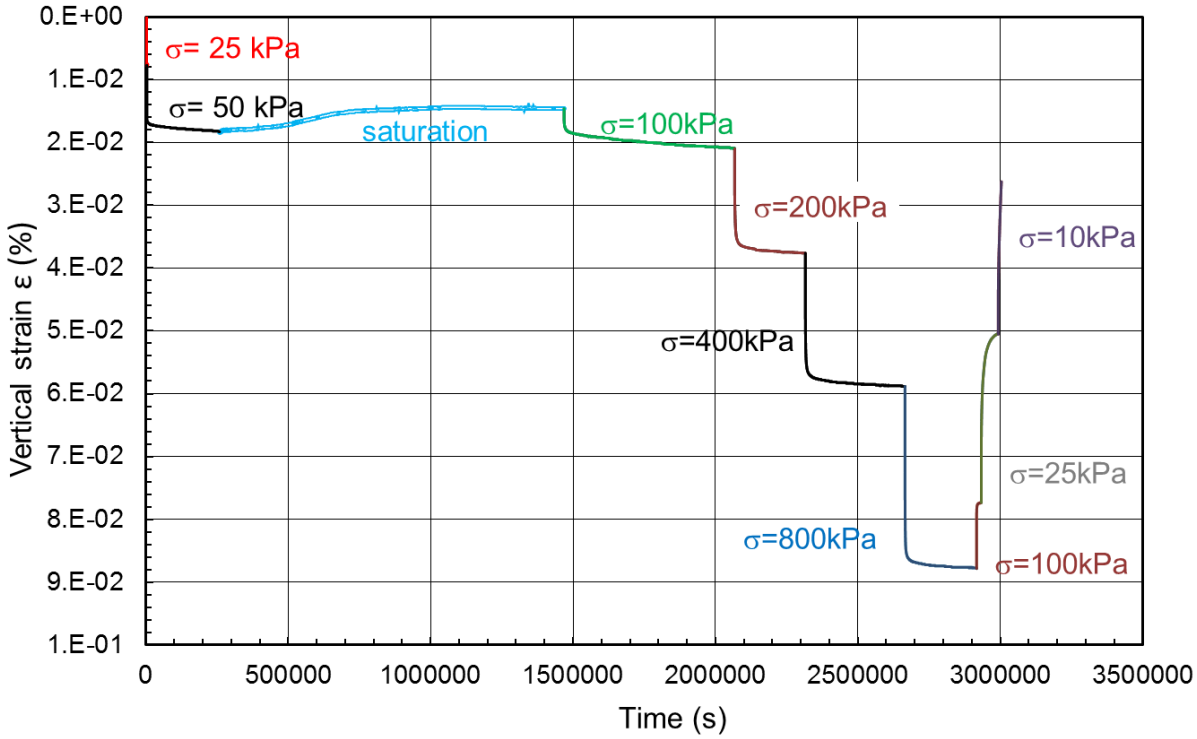

Figure 4.17. Vertical strain vs time for sand/bentonite (80/20) OE2 conventional oedometer test

It is observed in Figure 4.18 a compression before saturation stage, and an increase of volume after soaking, returning to its initial volume. When the unloading is exerted, the sample drastically swell increasing its initial volume, it is not a coincidence that the sample with the greater dry density presents a higher swelling behaviour.

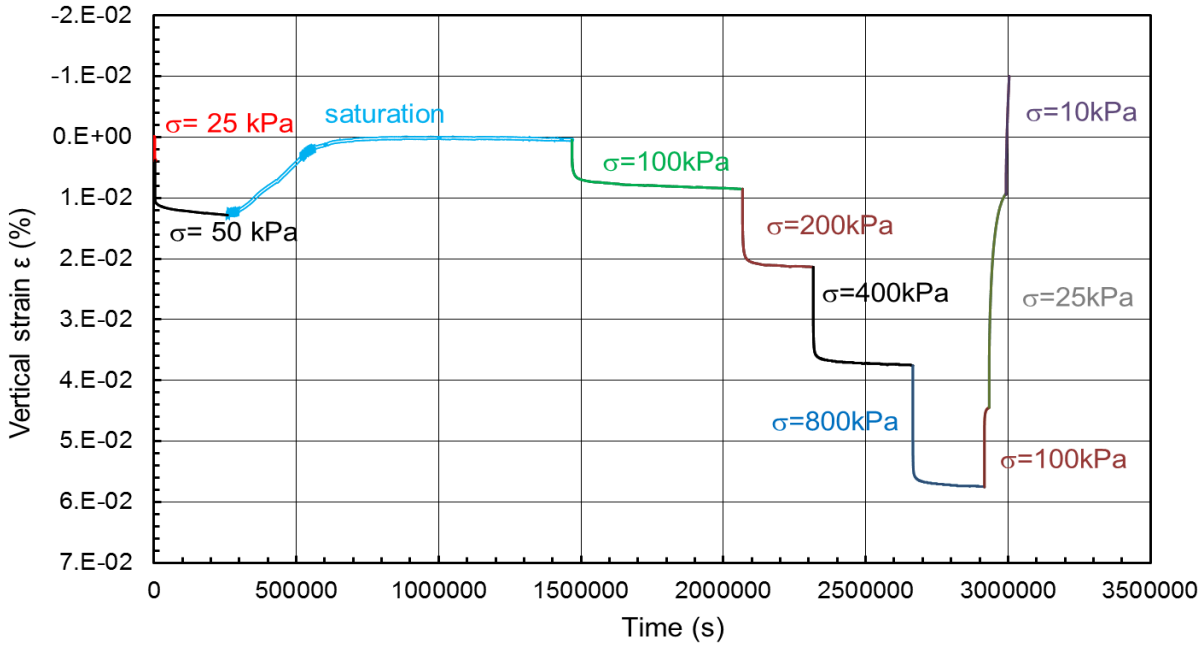

Figure 4.18. Vertical strain vs time for sand/bentonite (80/20) OE3 conventional oedometer test

The void ratio vary according to stage of loading or unloading of the sample. In Figure 4.19 a leap in the results is shown, when saturation of the sample occurs having the same load.

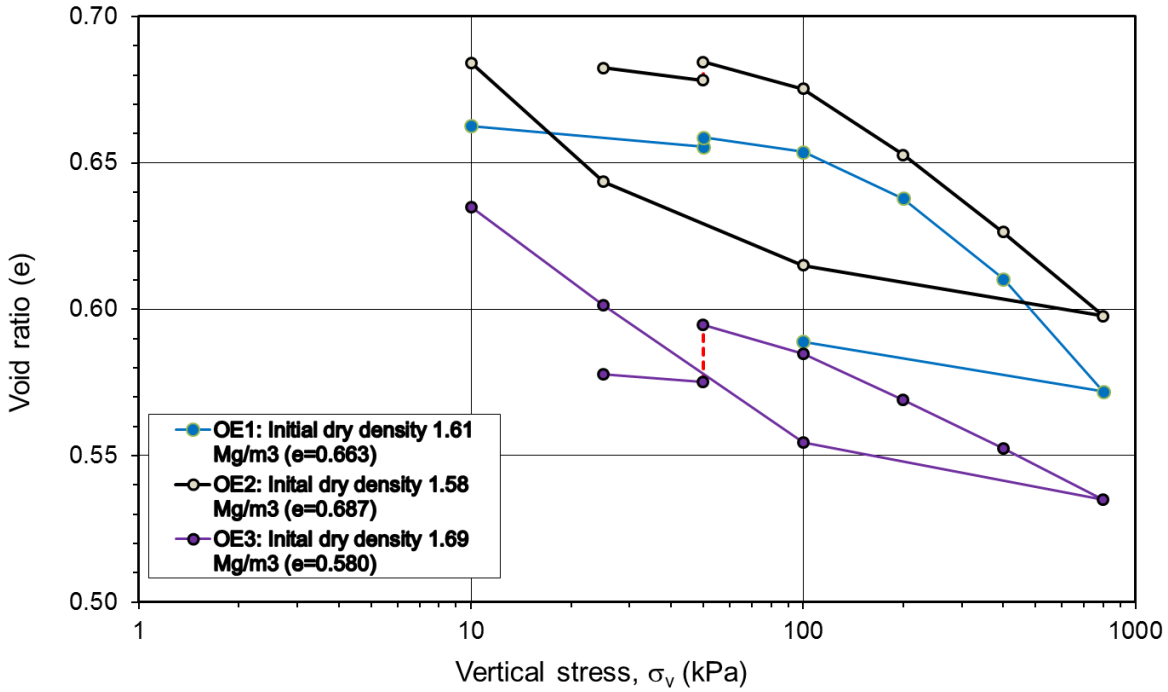

Figure 4.19. OE1, OE2, OE3, compression curve

A summary with the properties is presented in Table 4.9. In this table the secondary consolidation coefficient for OE3 is constant after applying 200 kPa, this could be because the sample needed more time to produce those settlements under the following loads.

Table 4.9. Summary of the properties OE2, OE3 under loads

Load step	Average void ratio e		Cv (m^2/s)		Em (MPa)		Cα		Water conductivity K (m/s)	
	OE2	OE3	OE2	OE3	OE2	OE3	OE2	OE3	OE2	OE3
50 - 100	0.59	0.68	4.90E-09	1.00E-08	13	25	0.0011	0.0009	3.71E-12	4.00E-12
100 - 200	0.577	0.664	7.00E-09	6.80E-09	13	9	0.0011	0.0015	5.60E-12	7.39E-12
200 - 400	0.561	0.64	1.35E-08	1.00E-08	25	16	0.0011	0.0015	5.48E-12	6.25E-12
400 - 800	0.544	0.612	2.00E-08	1.50E-08	48	29	0.0011	0.0015	4.21E-12	5.17E-12

Figure 4.20 shows a comparison of water conductivities obtained by the conventional oedometers with sand/bentonite (80/20) and Manca (2015). The results obtained by OE1, OE2 and OE3 are lower.

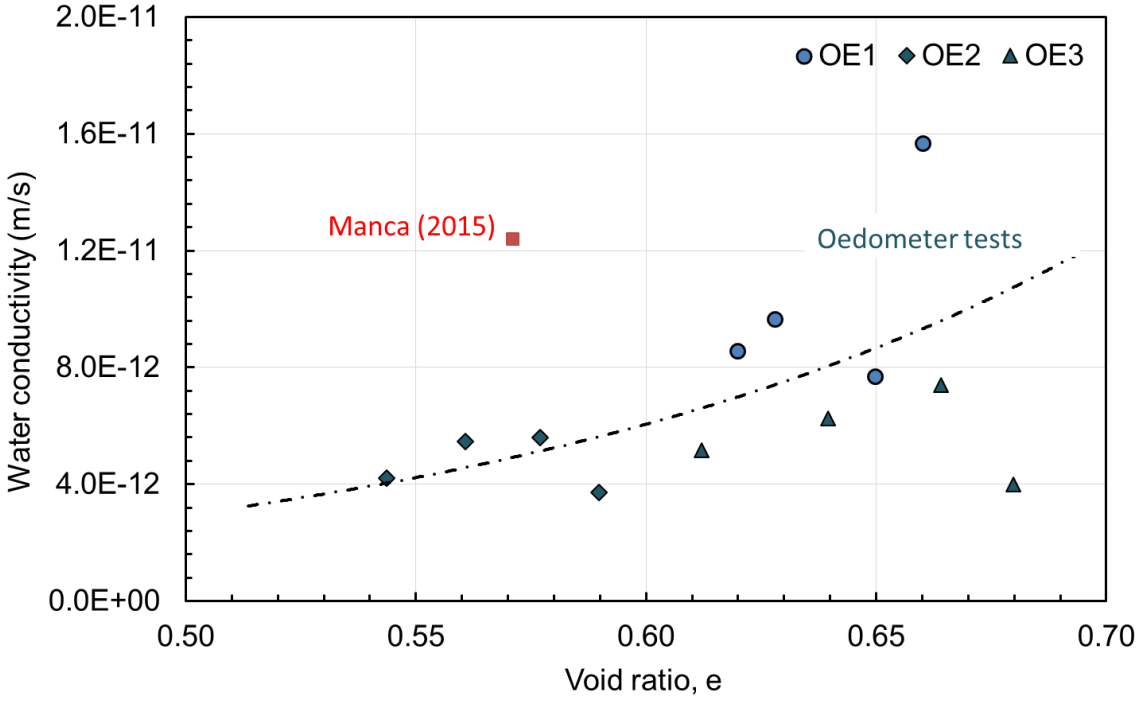

Figure 4.20. Comparison of water conductivities sand/bentonite (80/20)

4.4 Swelling tests under constant volume conditions

The initial conditions obtained from testing the MX-80 bentonite and sand/bentonite (80/20) are the same conditions considered for the MU-B tests.

4.4.1 MX-80 bentonite

The swelling pressure for the MX-80 is evaluated under saturated and constant volume conditions with respect to time presented in Figure 4.21. The initial conditions are shown in Table 4.10. After seven days of the material being tested the swelling pressure is stabilised at 249 kPa. The values obtained by the load cell were filtered to reduce the noise in them.

Table 4.10. Initial conditions for swelling tests for MX-80 bentonite

Test	1
Initial water content (%)	70.58
Bulk density (Mg/m³)	1.48
Dry density (Mg/m³)	0.87
Void ratio	2.15
Degree of saturation	0.90
Specific Gravity*	2.74

*Seiphoori (2015)

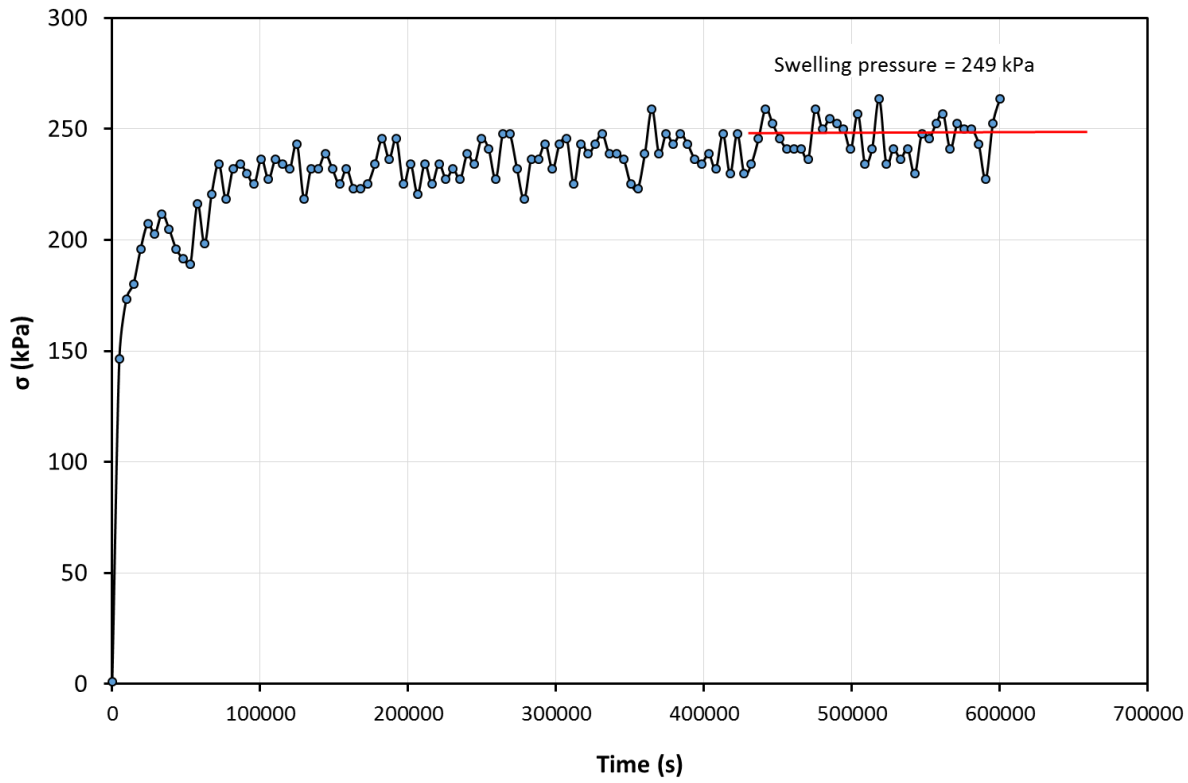

Figure 4.21. Swelling pressure developed through time for MX-80 bentonite

4.4.2 Sand/bentonite (80/20)

In Figure 4.22 it shows the development of the swelling pressure. Furthermore, in Table 4.11 the initial conditions are presented. The swelling pressure value is 200 kPa obtained in an oedometer with load arm.

Table 4.11. Initial conditions for swelling tests for Sand/bentonite (80/20) oedometer with load arm

Test	2
Initial water content (%)	11.58
Bulk density (Mg/m³)	1.80
Dry density (Mg/m³)	1.61
Void ratio	0.648
Degree of saturation	0.46
Specific Gravity±	2.67

±Manca, 2015

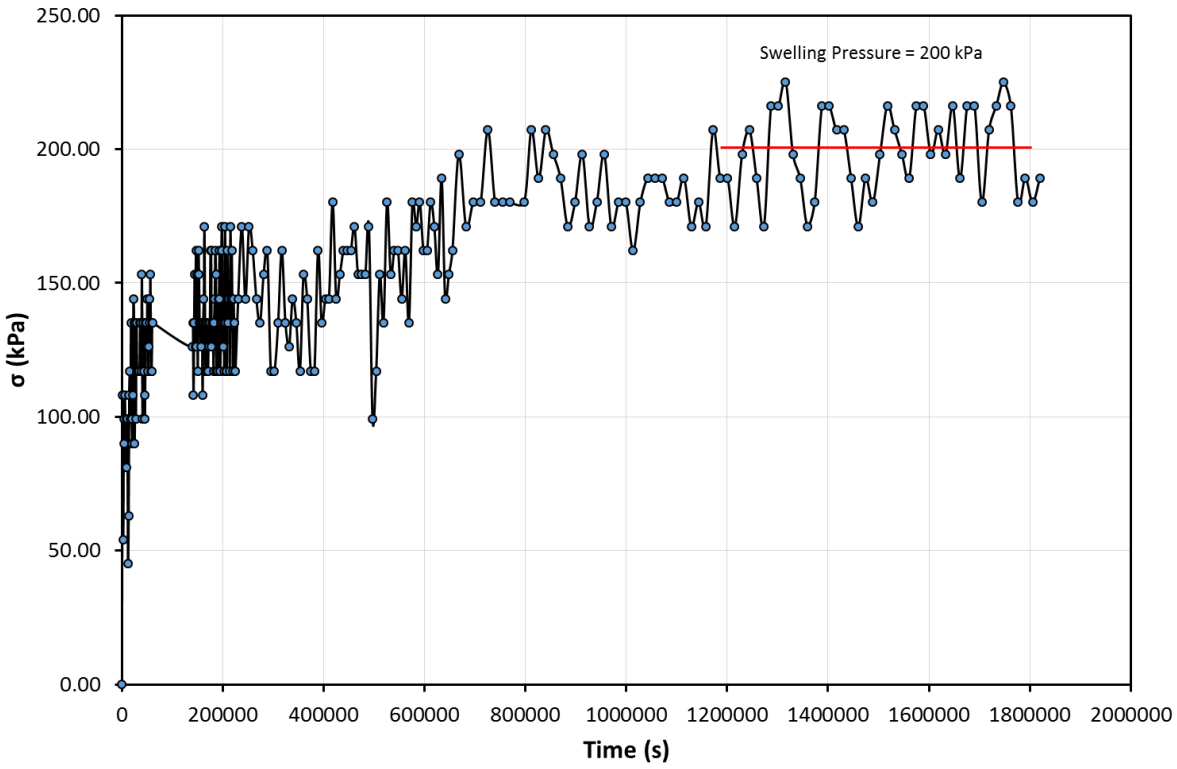

Figure 4.22. Swelling pressure developed through time for sand/bentonite (80/20) oedometer with load arm

A comparison between a test done to the sand/bentonite (80/20) by an oedometer with load arm and a test done only with the load cell is presented in Figure 4.23. The initial conditions for the test exerted only with the load cell are shown in Table 4.12.

Table 4.12. Initial conditions for swelling tests for Sand/bentonite (80/20) oedometer with load cell

Test	3
Initial water content (%)	13.33
Bulk density (Mg/m³)	1.86
Dry density (Mg/m³)	1.67
Void ratio	0.59
Degree of saturation	0.60
Specific Gravity±	2.67

±Manca, 2015

In spite of the dry density is greater with the sample tested in the load cell (test 3) than the sample tested in an oedometer with load arm (test 2), the values of swelling pressure are reduced in the test 3. This occurs due to the water content, which is bigger in the test 3 than in the test 2.

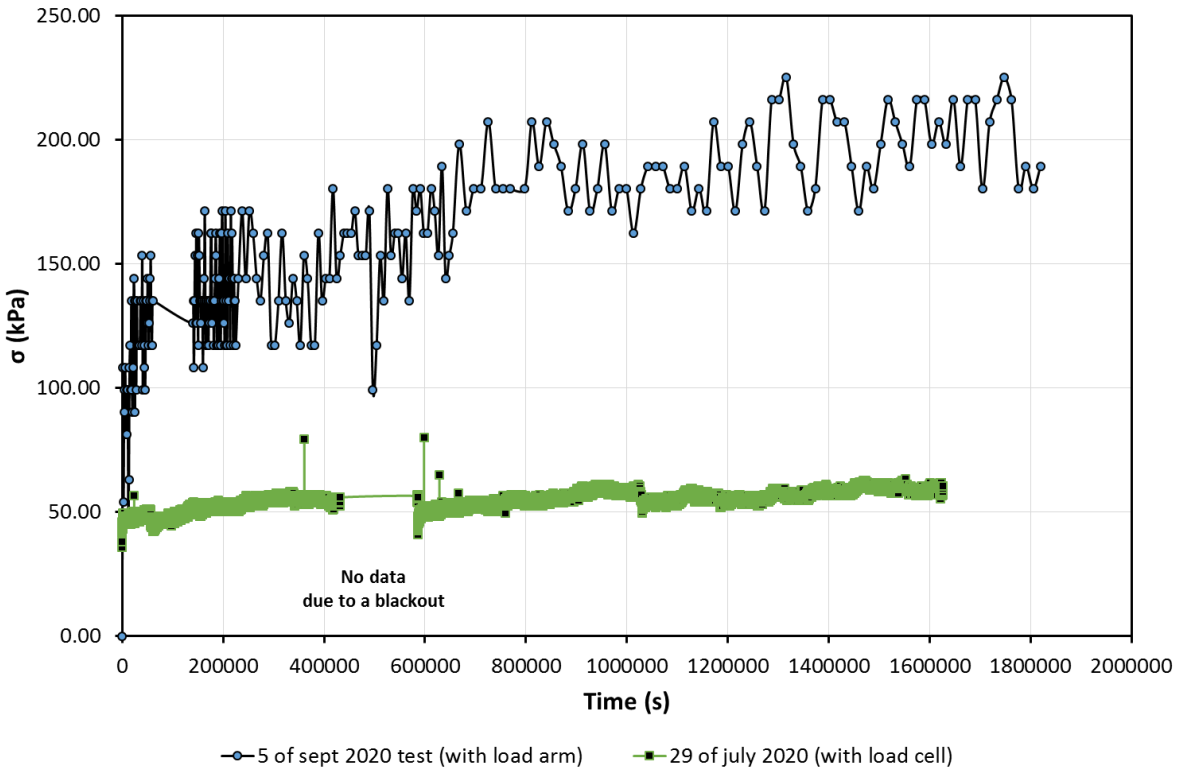

Figure 4.23. Swelling tests comparison sand/bentonite (80/20)

4.4.3 Water conductivity

From the swelling tests using an oedemeter with a load arm testing the sand/bentonite (80/20), it is obtained the water conductivity through Darcy's law. The equations used are listed below and the Figure 4.24 has a scheme with dimensions used to determine the water conductivity.

$$Q = KiA \tag{2}$$

$$i = \frac{\Delta h}{\Delta L} \tag{3}$$

Q = rate of flow
K = water conductivity
A = cross sectional area of the soil sample
i = hydraulic conductivity
Δh= total fluid potential
Δl = length of the soil sample

The result of the water conductivity was 3.34×10^{-11} m/s. This result is greater than the results obtained by Manca (2015), which was 1.2×10^{-11} m/s.

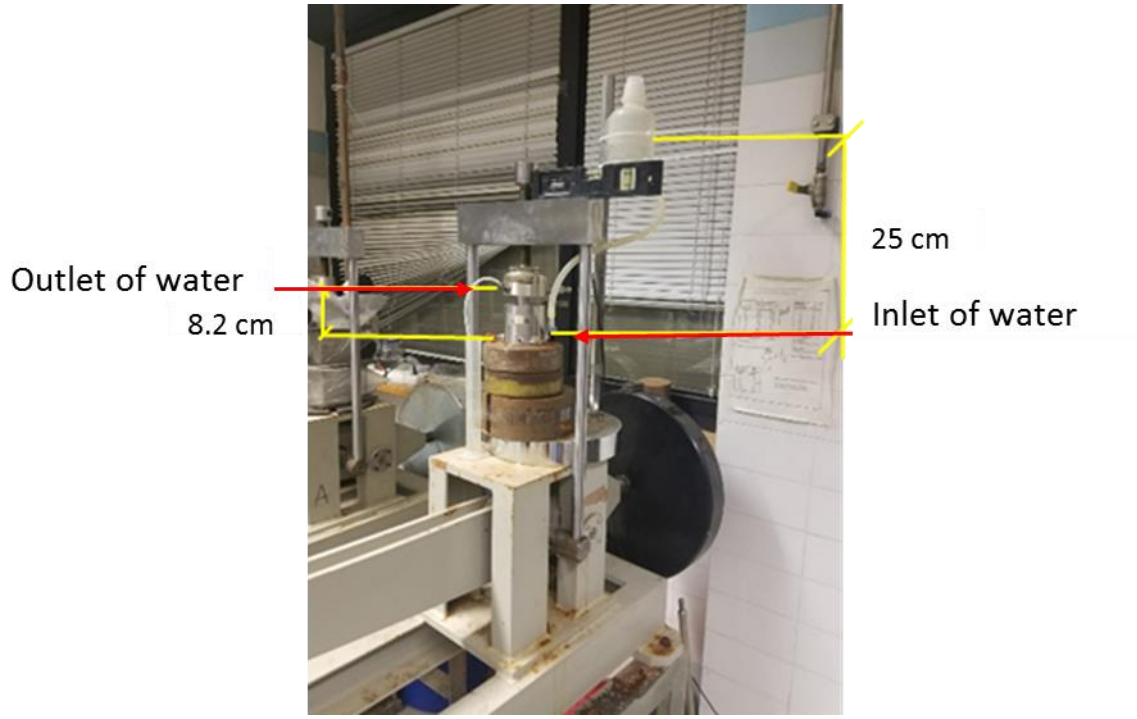

Figure 4.24. Scheme to determine the water conductivity sand/bentonite (80/20)

4.5 Water retention curve

The total suction of the MX-80 bentonite is measured and presented in Table 4.13. For this material only two tests have been made. It is appeared after a higher water content the material still have a significant suction.

Table 4.13. Results for the measurements of the total suction MX-80 bentonite

Test	S1	S2
Compaction energy (kJ/m^3)	647	647
Initial water content (%)	70.49	83.06
Bulk density (Mg/m^3)	1.56	1.49
Dry density (Mg/m^3)	0.92	0.82
Void ratio	1.99	2.36
Degree of saturation	0.97	0.97
Specific Gravity*	2.74	2.74
Total suction (kPa)	150	124

* Seiphoori, 2015

Nevertheless, for the sand/bentonite (80/20) seven test have been carried out. In Table 4.14 are presented. In addition in Figure 4.25 and Figure 4.26 the water retention behaviour are presented.

The points on the water retention curves started from a total suction of 200 kPa with 11% of water content. Then, while the sample is saturated, the suction material is decreasing its value. Comparing the results obtained, it is notable that the mixture sand/bentonite has a low retention capacity, than the pure bentonite. This occurs because of the amount of sand in the mixture and to the microstructural characteristics of the pure bentonite. From these results and other works (Manca, 2015; Seiphoori, 2015, et al.) can be inferred a lower dependency of the suction in the dry densities.

Table 4.14. Results for the measurements of the total suction sand/bentonite (80/20)

Test	S1	S2	S3	S4	S5	S6	S7
Compaction energy (kJ/m³)	266	304	342	837	875	875	685
Initial water content (%)	11.66	11.43	11.67	13.88	18.51	23.6	27.04
Bulk density (Mg/m³)	1.54	1.62	1.74	1.83	1.86	2.00	1.94
Dry density (Mg/m³)	1.38	1.44	1.56	1.61	1.57	1.62	1.52
Void ratio	0.93	0.85	0.71	0.66	0.70	0.65	0.75
Degree of saturation	0.33	0.36	0.44	0.56	0.71	0.97	0.96
Specific Gravity ±	2.67	2.67	2.67	2.67	2.67	2.67	2.67
Total suction (kPa)	222	210	215	63	11	6	4.1

±Manca, 2015

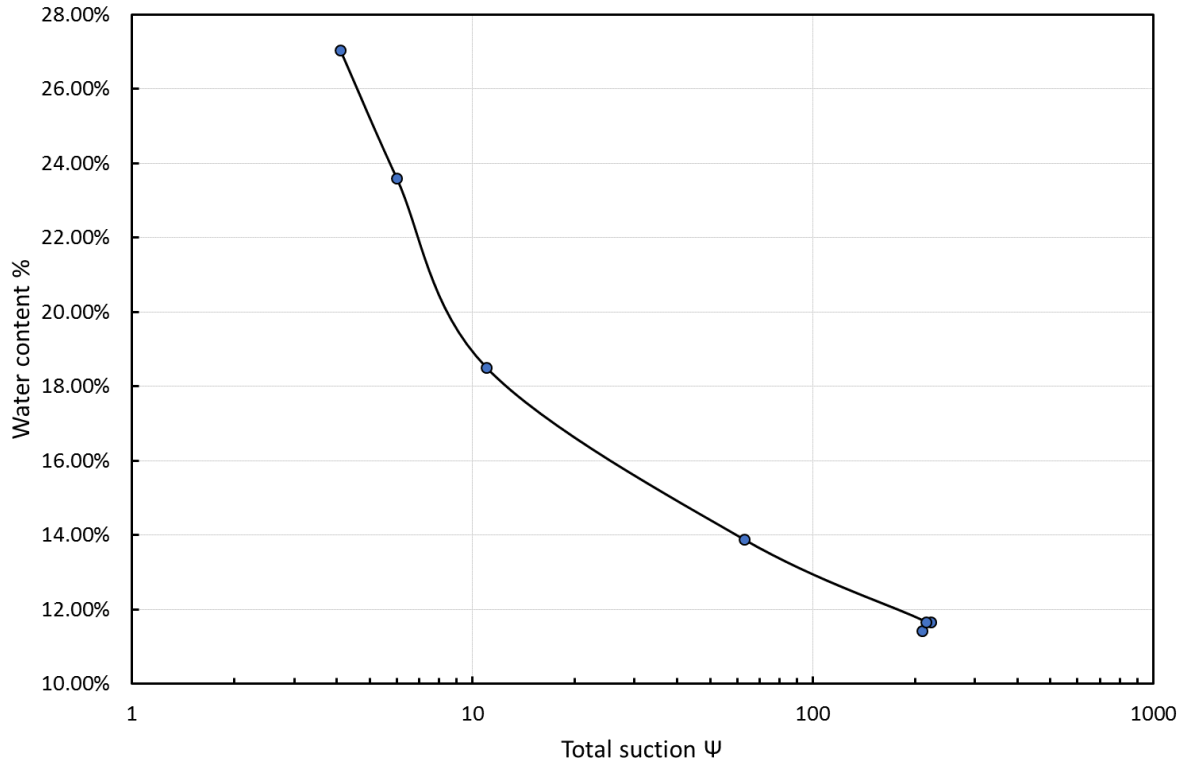

Figure 4.25. Water retention curve of sand/bentonite (80/20) water content vs total suction

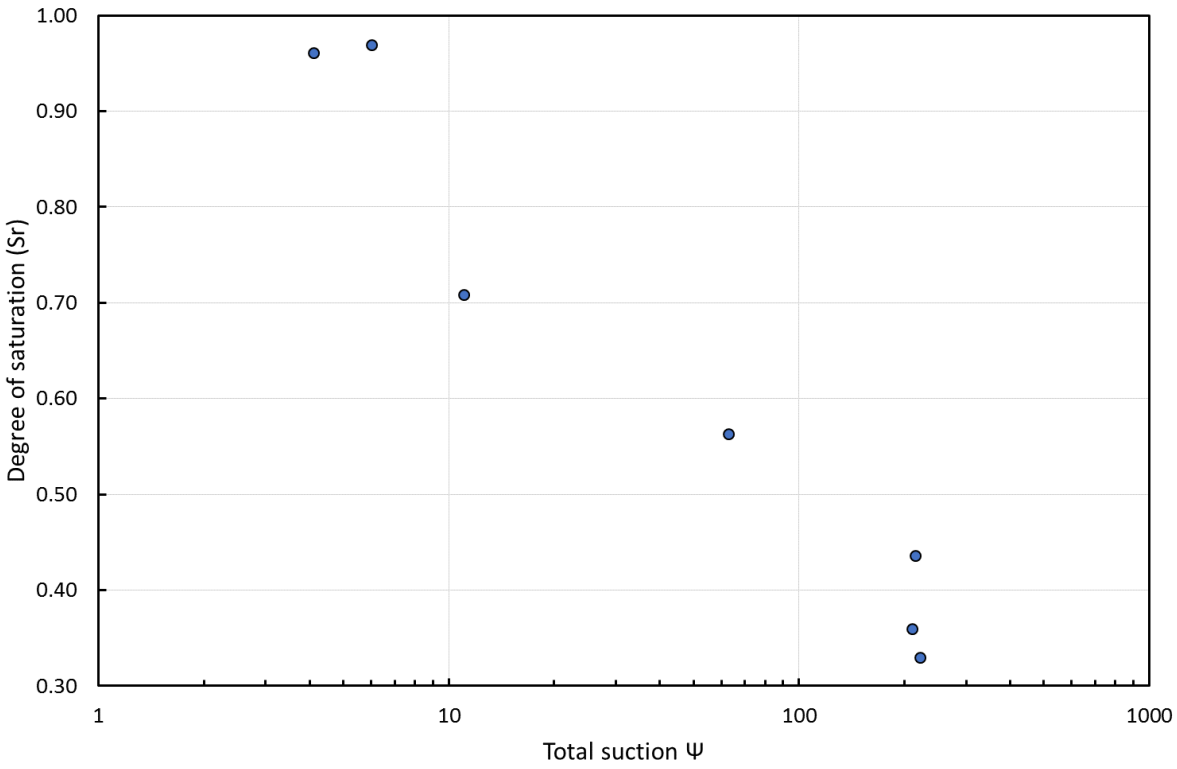

Figure 4.26. Water retention curve of sand/bentonite (80/20) degree of saturation vs total suction

5 Conclusions

The present investigation was aimed at characterising and understanding the hydro-mechanical behaviour of the Wyoming granular bentonite and mixture sand/bentonite (80/20) with the purpose to find a methodology to place these materials in a mock up (MU) test, where transport with distilled water and gas tests will be carried out.

The basic properties of the materials were obtained. Grain size distribution, Atterberg limits and hygroscopic water content were determined. A compilation of porosimetry from two works Seiphoori (2015) and Manca (2015) were gathered together in this framework. Both works for MX-80 bentonite and for sand/bentonite (80/20) presents a bimodal structure (with macropores and micropores) when the samples are unsaturated compacted. While the MX-80 bentonite gets saturated, this bimodal structure starts changing by decreasing the macropores and increasing the micropores. In sand/bentonite (80/20) tests the macropores are reduced when the sample is wetted but the bimodal structure still exists. This can be related to a slight variations on the distribution of the sand and bentonite grains. The mixture change its structure, decreasing the macropores, when it is wetted under constant volume conditions.

Standard proctor tests were carried out in order to determine the optimum water content and the target dry density of the sand/bentonite (80/20). The greater the energy was applied, the higher the dry density obtained and the lower the void ratio gets.

In addition, conventional oedometer tests and swelling tests under constant volume were made for both MX-80 bentonite and sand/bentonite (80/20). The values of the initial degree of saturation in the pure bentonite tested imply the presence of suction. The large values of voids obtained in this test are due to the minerals of montmorillonite. The swelling strain, in conventional oedometer tests, is larger in those samples with lower water content because they can adsorb more water in their crystalline lattice.

Regarding the S/B mixture, oedometer test results show that the vertical strain for the sample at hygroscopic water content is lower than in other tests. This can be explained by the fact that the material exceeds the pre-consolidation load, and also that the material was compacted by the dry side of the compaction curve. The test with the optimum water content and higher dry density present the larger vertical strain. The water conductivities were theoretically obtained in these tests.

The results of swelling tests describe a larger swelling pressure for the material MX-80 bentonite. The swelling pressure of the sand/bentonite (80/20) can be produced by the accommodation of the

particles of sand breaking the structure of the bentonite. The water conductivity was obtained for the mixture in this test by Darcy's Law.

Furthermore, suction tests were done by means of a tensiometer. The results revealed that for the MX-80 bentonite with higher water content, the material still has a significant suction. On the contrary, the sand/bentonite (80/20) has less water storage capacity, reaching a total saturation with less amount of water.

In order to determine the methodology to emplace the material inside the cell MU-B, a trial layer fabrication and sand/bentonite mixture installation were carried out. 3D printed moulds were design and carefully used to control the density of the material during compaction. Paraffin tests were done to samples taken at different locations and depth. The methodology executed in the third trial layer compaction test was the most effective. The temperature and relative humidity of the zone near the equipment need to be measured and controlled to avoid the material gets dry. It has been concluded that for future tests these parameters will be controlled by placing an industrial plastic curtain in all the perimeter of work, a humidifier to maintain the relative humidity, and sensors of temperature. The material will be weighted, prepared, and emplaced in the perimeter of the work zone where the equipment is located.

Ensuring that the mixture sample complies with the defined initial conditions of density at all points inside the MU-B cell, it is considered a highlighted issue to achieve the final objective of the gas test. This due to the gas could take a preferential path if there would be a less densified area, and that would interfere with a correct analysis of the results.

Finally, this investigation contributes adding information about the characterisation and hydro-mechanical behaviour of Wyoming granular bentonite and sand/bentonite (80/20). However, more tests are required to compare and verify the parameters obtained. In this case, a column infiltration should be made to verify the water conductivity, moreover, it is recommended to obtain the water retention curve with samples with the same dry density.

6 References

Akinwunmi, B., Sun, L., Hirvi, J. T., Kasa, S., & Pakkanen, T. A. (2019). Influence of temperature on the swelling pressure of bentonite clay. *Chemical Physics*, *516*(June 2018), 177–181. https://doi.org/10.1016/j.chemphys.2018.09.009

Cui, Y. (2017). On the hydro-mechanical behaviour of MX80 bentonite-based materials. *Journal of Rock Mechanics and Geotechnical Engineering*, *9*(3), 565–574. https://doi.org/10.1016/j.jrmge.2016.09.003

Hoffmann, C., Alonso, E. E., & Romero, E. (2007). Hydro-mechanical behaviour of bentonite pellet mixtures. *Physics and Chemistry of the Earth*, *32*(8–14), 832–849. https://doi.org/https://doi.org/10.1016/j.pce.2006.04.037

Imbert, C., & Villar, M. V. (2006). *Hydro-mechanical response of a bentonite pellets / powder mixture upon infiltration*. *32*, 197–209. https://doi.org/10.1016/j.clay.2006.01.005

Kale, R. C., & Ravi, K. (2019). Influence of thermal history on swell pressures of compacted bentonite. *Process Safety and Environmental Protection*, *123*, 199–205. https://doi.org/10.1016/j.psep.2019.01.004

Lloret, A., Villar, M. V., Sánchez, M., Gens, A., Pintado, X., & & Alonso, E. E. (2003). Mechanical behaviour of heavily compacted bentonite under high suction changes. *Géotechnique*, *53*(1), 27–40. https://doi.org/https://doi.org/10.1680/geot.53.1.27.37258

Manca, D. (2015). *Hydro-chemo-mechanical characterisation of sand / bentonite mixtures , with a focus on the water and gas transport properties* (Vol. 6790). École Polytechnique Fédérale de Lausanne.

Montañez, J. E. (2002). *Suction and volume changes of compacted sand-bentonite mixtures.* University of London (Imperial College of Science, Technology and Medicine).

Perez, N. (2008). *Determinación de curvas características en suelos no saturados con celdas de presión*. Retrieved from http://www.imt.mx/archivos/Publicaciones/PublicacionTecnica/pt313.pdf

Proia, R., Croce, P., & Modoni, G. (2016). Experimental investigation of compacted sand-bentonite mixtures. *VI ITALIAN CONFERENCE OF RESEARCHERS IN GEOTECHNICAL ENGINEERING –Geotechnical Engineering in Multidisciplinary Research: From Microscale to Regional Scale, CNRIG2016. Procedia Engineering*, *158*, 51–56. https://doi.org/https://doi.org/10.1016/j.proeng.2016.08.404

Romero, E. (2013). A microstructural insight into compacted clayey soils and their hydraulic properties. *Engineering Geology*, *165*, 3–19. https://doi.org/10.1016/j.enggeo.2013.05.024

Seiphoori, A. (2015). Thermo-hydro-mechanical characterisation and modelling of Wyoming granular bentonite. *Nagra (National Cooperative for the Disposal of Radioactive Waste): Techbical Report 15-05, 5430*. https://doi.org/https://doi.org/10.13140/RG.2.2.13266.25281

Sellin, P., & Leupin, O. X. (2013). The Use of Clay as an Engineered Barrier in Radioactive-Waste Management a Review. *Clays Clay Miner*, *61*(6), 477–498. https://doi.org/https://doi.org/10.1346/CCMN.2013.0610601

Smellie, J., & AB, C. (2001). Evidence from the geological record to evaluate the suitability of

bentonite as a buffer material during the long-term underground containment of radioactive wastes. In *SKB Technical Report (TR-01-26)*. Retrieved from https://www.skb.com/publication/19067

Sutherland, W. M., & Drean, T. (2014). *Wyoming bentonite: Summary report:* Retrieved from https://hdl.handle.net/20.500.11919/5045

Villar, M. V., & Lloret, A. (2008). *Influence of dry density and water content on the swelling of a compacted bentonite*. *39*, 38–49. https://doi.org/10.1016/j.clay.2007.04.007

Villar, M. V. (2005). MX-80 Bentonite. Thermo-Hydro-Mechanical Characterisation Performed at CIEMAT in the Context of the Prototype Project. *Informes Técnicos Ciemat 1053 (2001-2004)*, 146.

Villar, M. V, & Lloret, A. (2010). Experimental investigation into temperature effect on hydro-mechanical behaviours of bentonite. *Journal of Rock Mechanics and Geotechnical Engineering*, *2*(1), 71–78. https://doi.org/10.3724/SP.J.1235.2010.00071

Wang, Q., Minh, A., Cui, Y., & Delage, P. (2013). The effects of technological voids on the hydro-mechanical behaviour of compacted bentonite – sand mixture. *Soils and Foundations*, *53*(2), 232–245. https://doi.org/10.1016/j.sandf.2013.02.004

7 Appendix

PROCTOR STANDARD

Sand/bentonite (80/20)

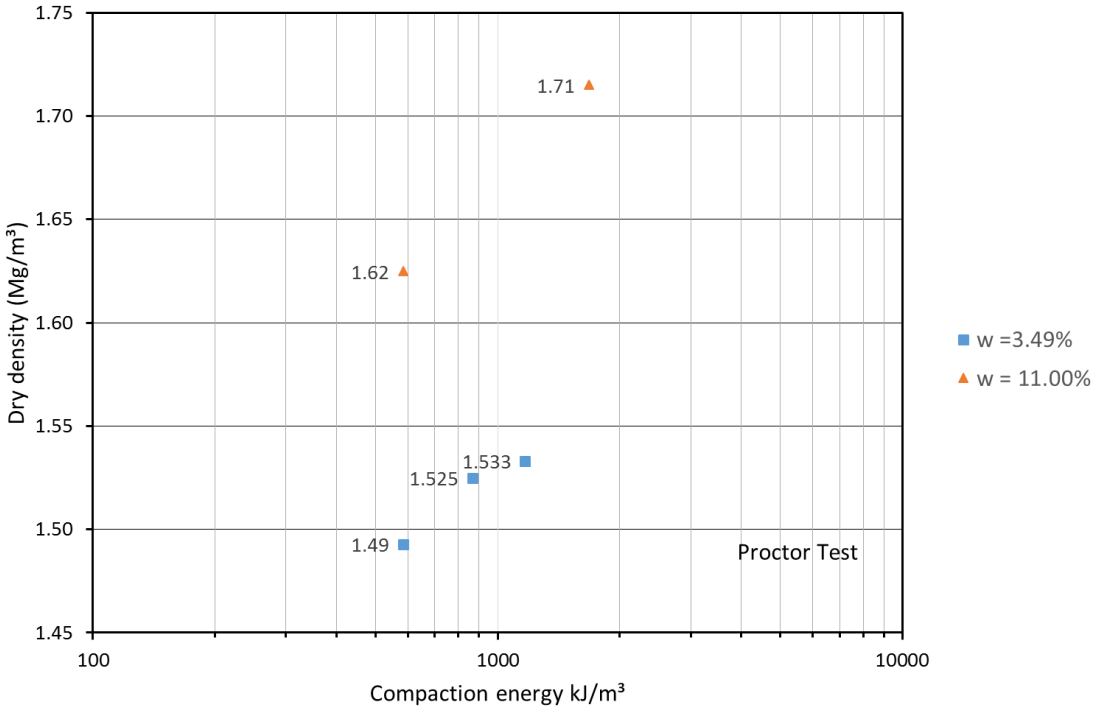

Comparison of energys and density between Proctor mould with optimum water content 11%, Manca (2015) and the Oedometric moulds prepared to measure the suction.

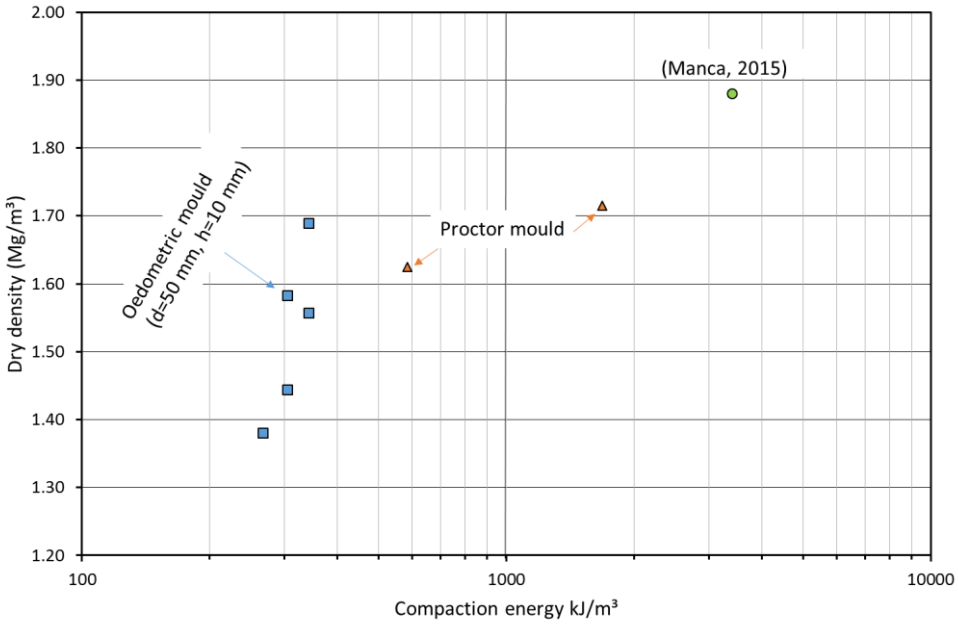

MU-B cell compaction layers

Sand bentonite (80/20) installed by dynamic compaction

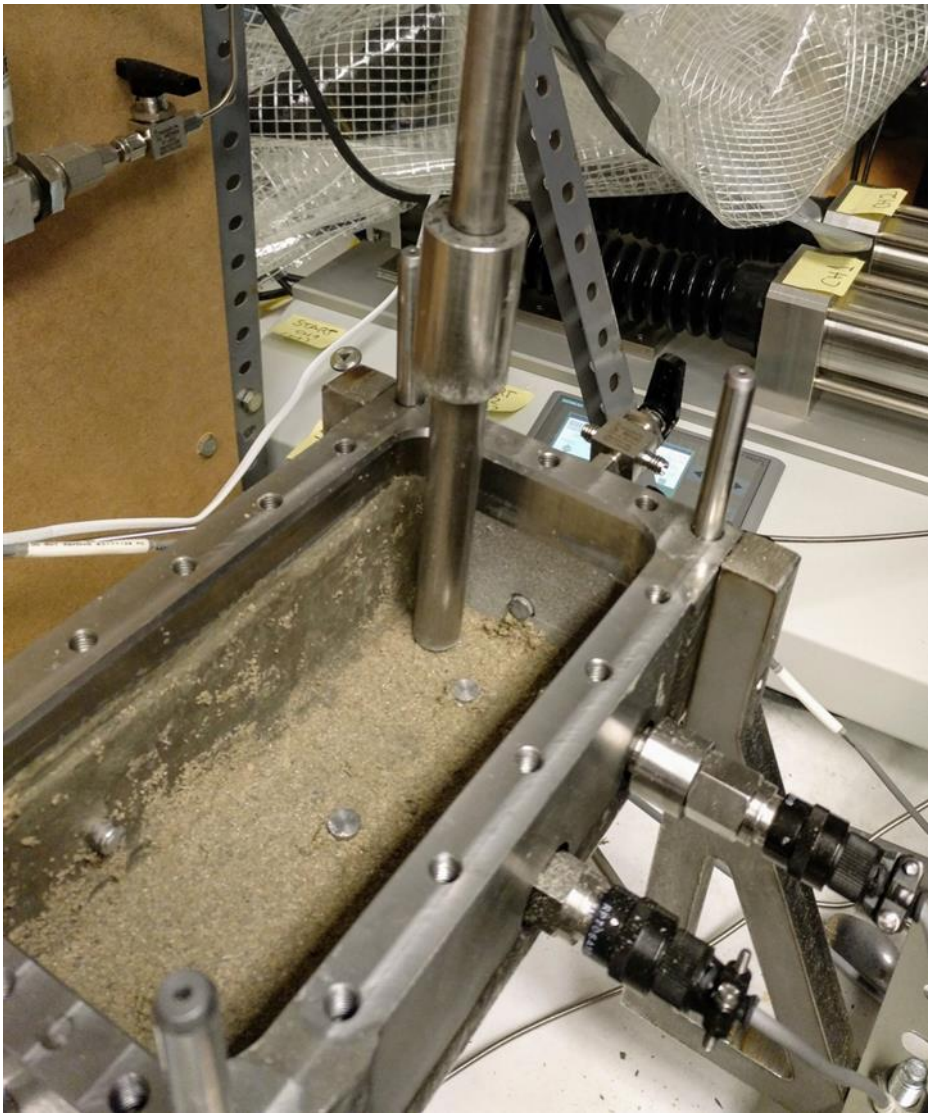

S/B before last compaction

After last compaction

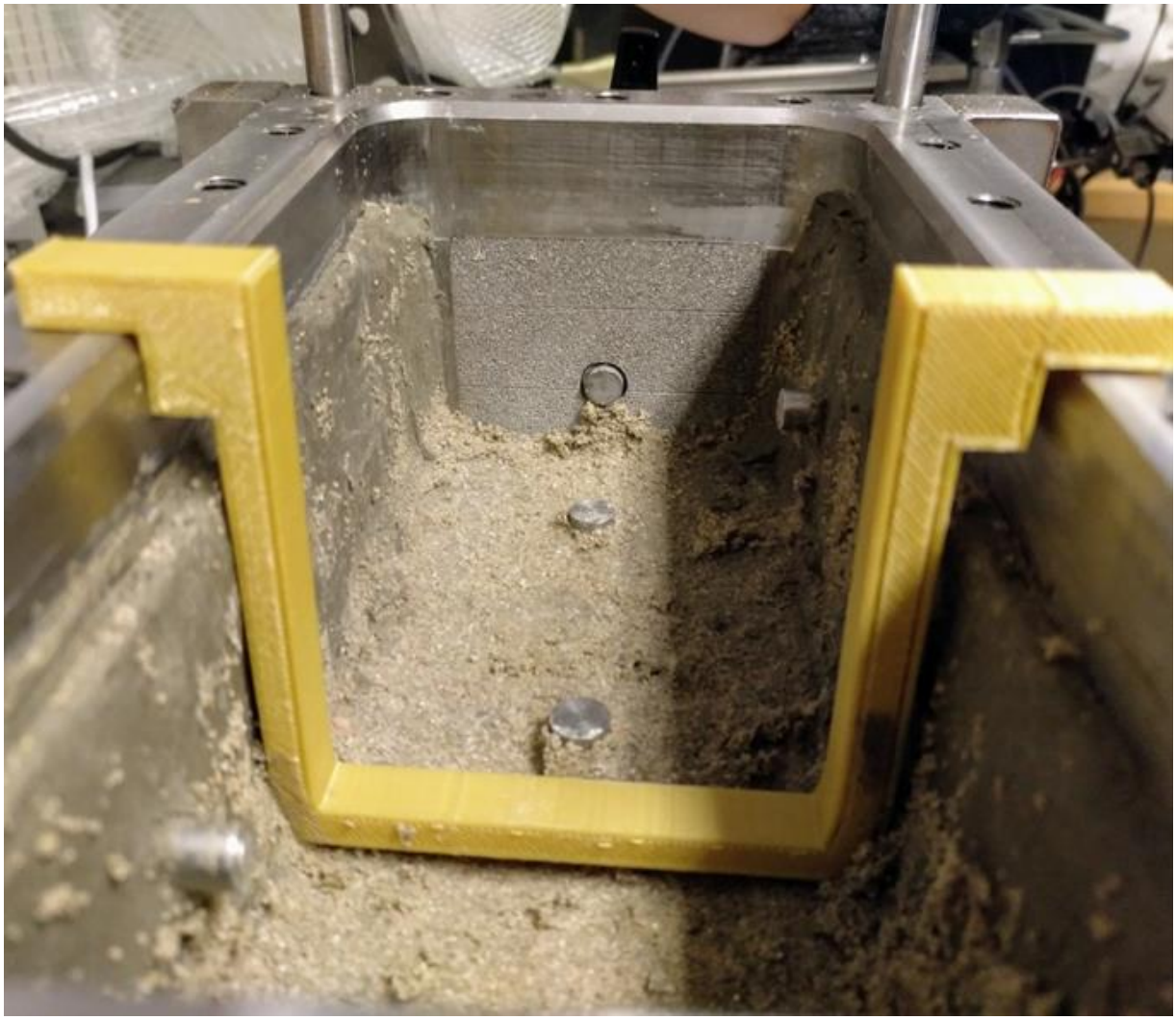

Layer Fabrication granular MX-80 bentonite

Layer Fabrication granular MX-80 bentonite

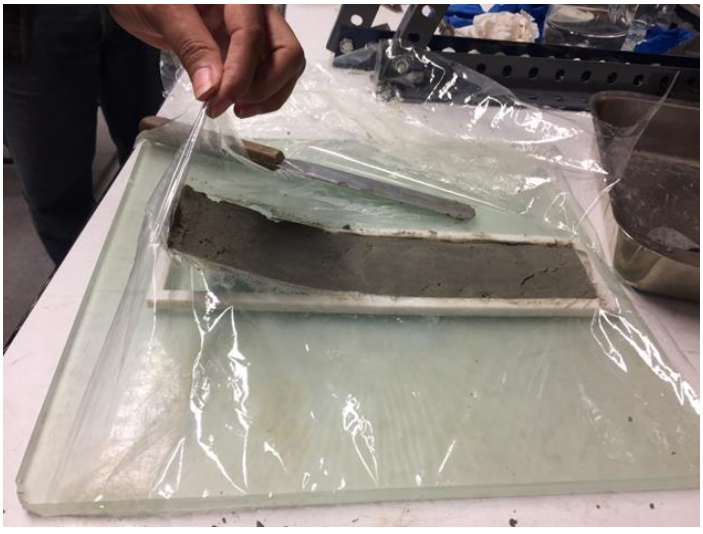

MU-B Equipment assembly

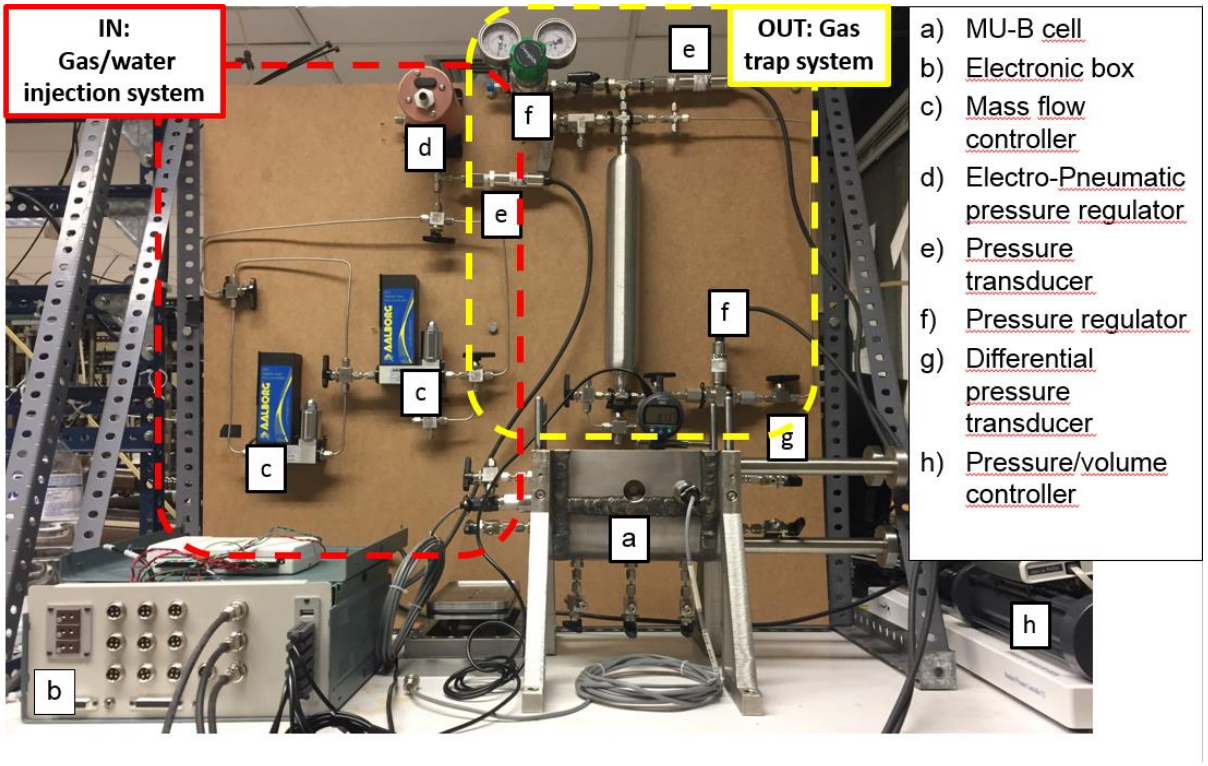

Oedometer Tests

Sand/bentonite (80/20)

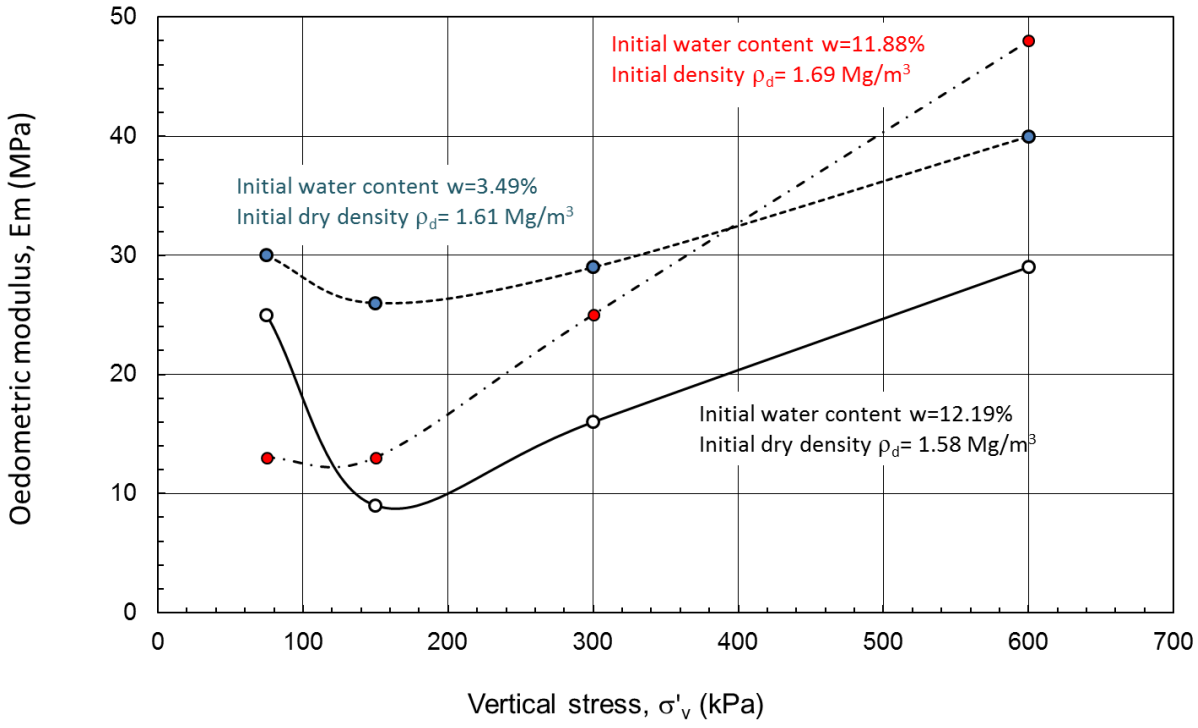

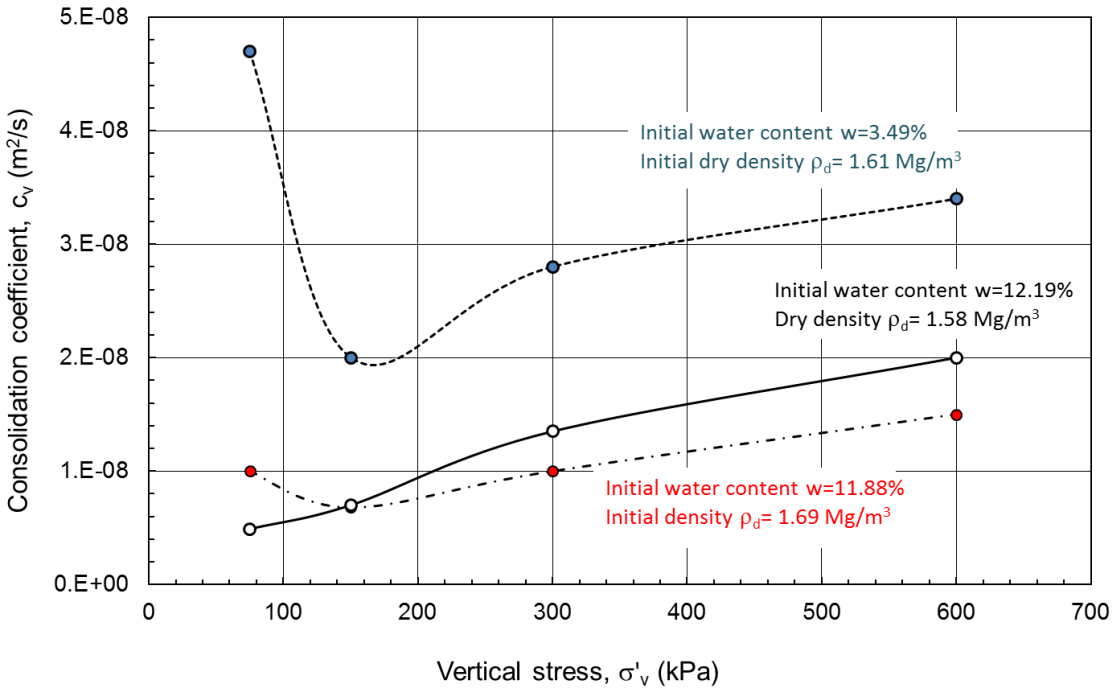

Oedometer Tests

Sand/bentonite (80/20)